and Bayne, 1999). Using a 1 mHz transducer, the probe simultaneously measures ultrasonic attenuation and speed.

Current slurry characterization techniques leave much to be desired, particularly at low solids concentrations. The Argonne ultrasonic probe has an error of over 50% at solids concentrations under 5 weight percent (Hylton 1999). This error is caused in large part by the presence of bubbles in the waste stream. The work presented in this study will show that when used properly ultrasound can give reliable data even in the presence of small amounts of gas.

2. Literature Review

Many researchers have performed theoretical and experimental work involving measuring and predicting speed and attenuation in multiphase mixtures. Since the focus of this paper is on experimental studies of multiphase systems literature involving experimental studies of multiphase systems will be discussed.

2.1 ATTENUATION:

Allegra and Hawley (1972) studied attenuation as a function of frequency in polystyrene particle-water systems. They studied particles ranging in radius from 0.044 to 0.635 microns, in the regime where thermal attenuation is the predominant phenomenon. In addition to reporting the data on attenuation these investigators also developed a theory.

Atkinson and Kytomaa (1991) measured attenuation and speed in clay-water and silica-water systems. The silica particles studies were of radius 500 μm, and volume fraction ranged from 0.05 to 0.6. The effective-medium approximation theory they

developed agreed well with their experimental data, except when $k_{cl}a$ became O(1) and multiple scattering effects become dominant.

Greenwood et al. (1993) studied attenuation in kaolin clay - water systems. They used a toneburst method where the system is interrogated by an ultrasonic signal of constant frequency. The frequency range studied was 0.5 to 3.0 MHz, and the maximum solid concentration was 44%. They found that for their system attenuation appeared to depend linearly on frequency over the range studied. Several different possible explanations are given for this behavior. The two given the most consideration to yield a linear relationship between attenuation and frequency are a combination of viscous and thermal attenuation or a hydrodynamic model which considers the increase in viscosity as the slurry becomes more concentrated.

Norato (1999) developed the experimental techniques used in this study to measure attenuation. Systems studied included polystyrene-water and various types of glass beads in water. Volume fractions studied ranged from 5% to 45%. Also studied was the effect of the presence of small amounts of gas on attenuation in solid-liquid systems.

Spelt et al. (2000) studied attenuation in polystyrene slurries and concentrated suspensions of glass particles. An effective medium theory was used to predict attenuation. Toneburst and Pulse/Fast Fourier Transform (FFT) methods were used to measure attenuation experimentally (Norato 1999). It was found that the theory matched the experiment well at volume fractions below 0.3.

2.2 SPEED

McClements and Fairley (1990) developed a technique to measure the speed of sound in a liquid. This method uses a dual reflection pulse-echo cell to cancel out any delay in the electronics, thus giving an excellent time-of flight measurement, accurate to ±0.3 m/s. McClements later (1991) employed a Fourier transform to determine ultrasonic speed as a function of frequency. These investigators used speed to determine (among other things) sugar contents in fruit juices. The method developed by McClements and co-workers was adopted for use in this study.

Tsouris et al. (1995) used a pulse-echo method to determine local volume fraction in liquid-liquid dispersions. A weighed average model, corrected for reflection and refraction, was used to predict volume fraction from time-of-flight measurements. No correction was made for delay in the monitoring equipment.

Cowan et al. (1998) used a method similar to McClements and co-workers to measure phase speed in systems of glass beads of average radius 0.438 mm. They studied the scattering regime with frequencies between 1 and 5 MHz and volume fractions from 0.21 to 0.61. An effective medium theory was employed which agreed well with the experimental data.

2.3 CONCLUSIONS

Considerable work has been performed studying ultrasonic attenuation in multiphase systems, both experimental and theoretical. Most experimental work studied systems of higher volume fraction particles, and little work has been done examining volume fractions under 5%. The work done by Norato (1999) proved that current theory

predicts attenuation well at low volume fraction but did not determine if reliable experimental data can be collected at low volume fraction. In addition, the systems studied were fairly ideal (monodisperse and very well characterized), and were not very representative of actual radioactive waste.

Ultrasonic speed work has concentrated on time-of flight measurements, generally ignoring dispersive effects, with the exception of the work done by McClements and co-workers and Cowen et Al. In addition, most speed experiments studied emulsions or other liquid-liquid systems. Little work has been done studying ultrasonic speed in solid-liquid systems or in systems with significant dispersive effects.

Accordingly, the purpose of the work in this study is twofold. The usefulness of attenuation in characterizing low volume fraction slurries will be determined. Since speed is more tolerant of changes in particle size than attenuation the usefulness of speed in characterizing low volume fraction slurries will also be determined.

3. Experimental

3.1 ATTENUATION BACKGROUND:

Attenuation as a function of frequency is measured for three systems: (a) soda-lime glass beads in water (referred to as the SLG system), (b) a physical radioactive waste slurry surrogate of Bentonite and kaolin clay in water (referred to as the BKC system), and (c) a chemical radioactive slurry surrogate consisting of a crystallized salt solution in supernate (referred to as the CSS system). The volume fraction range studied is approximately 0.005 to 0.1. Multiple replicates are performed to ensure reproducibility of data, and determine the error in the results.

The term 'attenuation" that has been used throughout this discussion is more appropriately called excess attenuation - that is, it is the additional attenuation of sound due to the presence of solids in the suspending liquid. Excess attenuation is determined by measuring the amplitude of the ultrasonic signal in the slurry (hereafter referred to as the sample reading) and comparing that to the amplitude of the ultrasonic signal in the pure liquid (referred to as the baseline reading). Since electrical transducers are used to create and measure the ultrasonic signal the amplitude is proportional to the voltage created by the transducer. Thus, for a given frequency and transducers d distance apart the attenuation is determined by:

$$\alpha = -\frac{1}{d}\ln\left(\frac{v_{slurry}}{v_{liquid}}\right) \qquad (1)$$

where v_{slurry} is the amplitude of the electrical signal produced by the transducers interrogating the slurry system and v_{liquid} is the amplitude of the electrical signal produced by the transducers interrogating the suspending liquid alone, with no solids present.

Two different methods are used to obtain voltage information at a specific frequency. The first method employs a spike pulse waveform followed by an FFT analysis. The other method uses a waveform of only one frequency (a toneburst). The voltages can then be read directly off of an oscilloscope and compared.

The spike pulse / FFT method as depicted in Figure 3.1 is by far the easier and more accurate way to measure attenuation. An ultrasonic pulse generator (Panametrics 5052PR) generates an electric pulse and sends it to the emitting transducer. The actuated

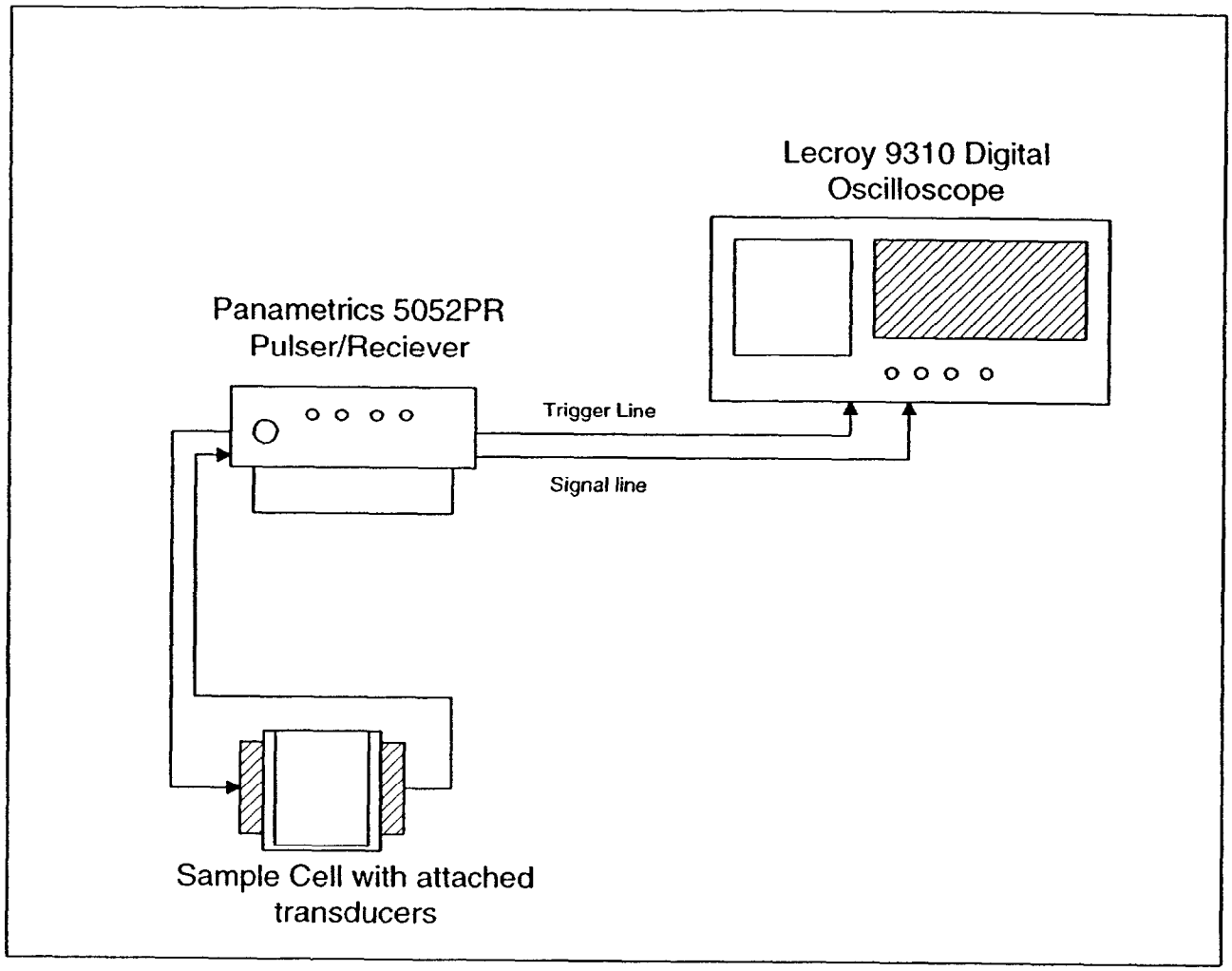

Figure 3.1: Schematic diagram of Pulse/FFT setup used to measure attenuation. A spike pulse is generated by the pulser/receiver and is transmitted to the transmitting transducer which is in contact with the sample. After traveling through the sample and being acquired by the receiving transducer the pulse is routed through the pulser/receiver to the oscilloscope.

emitting transducer transmits an acoustic pulse through the sample actuating the receiving transducer, where the signal is transmitted to and read by an oscilloscope (Lecroy 9310A). An FFT analysis of the amplitude is performed on the spike pulse, outputting voltage as a function of frequency for all of the component frequencies of the pulse. This procedure is performed both on the suspending liquid and the solid-liquid slurry. The voltages are used in eqn.1 to calculate the attenuation.

The toneburst method as depicted in Figure 3.2 is somewhat simpler in that no Fourier transforms are necessary, but is more tedious because an experiment needs to be run for each specific frequency for which a measurement is made. A computer controlled toneburst card (Matec TB1000) is used to generate a signal of a constant, specific frequency, and transmit that signal to the send transducer. Again, the signal actuates the emitting transducer, propagates through the sample, and actuates the receive transducer, where it is read by the oscilloscope. The peak-to-peak voltage of the signal is calculated and these values are used in eqn. 1 to calculate attenuation.

It is instructive to describe the method of data capture by the oscilloscope. In order to minimize error due to abnormal waveforms, and random noise, the oscilloscope actually takes an average of a certain designated number of spike pulses or toneburst sweeps before the FFT or amplitude calculation is made. The number of sweeps used to calculate the average is important because it determines the sampling time. If the sampling time is too long significant settling of the suspended solids in the test cell may occur, causing error due to appreciable variation of the actual suspended solids concentration in the test cell. If the number of sweeps taken is too small then random signal noise may be significant. This may be less of a problem in pipe slurry

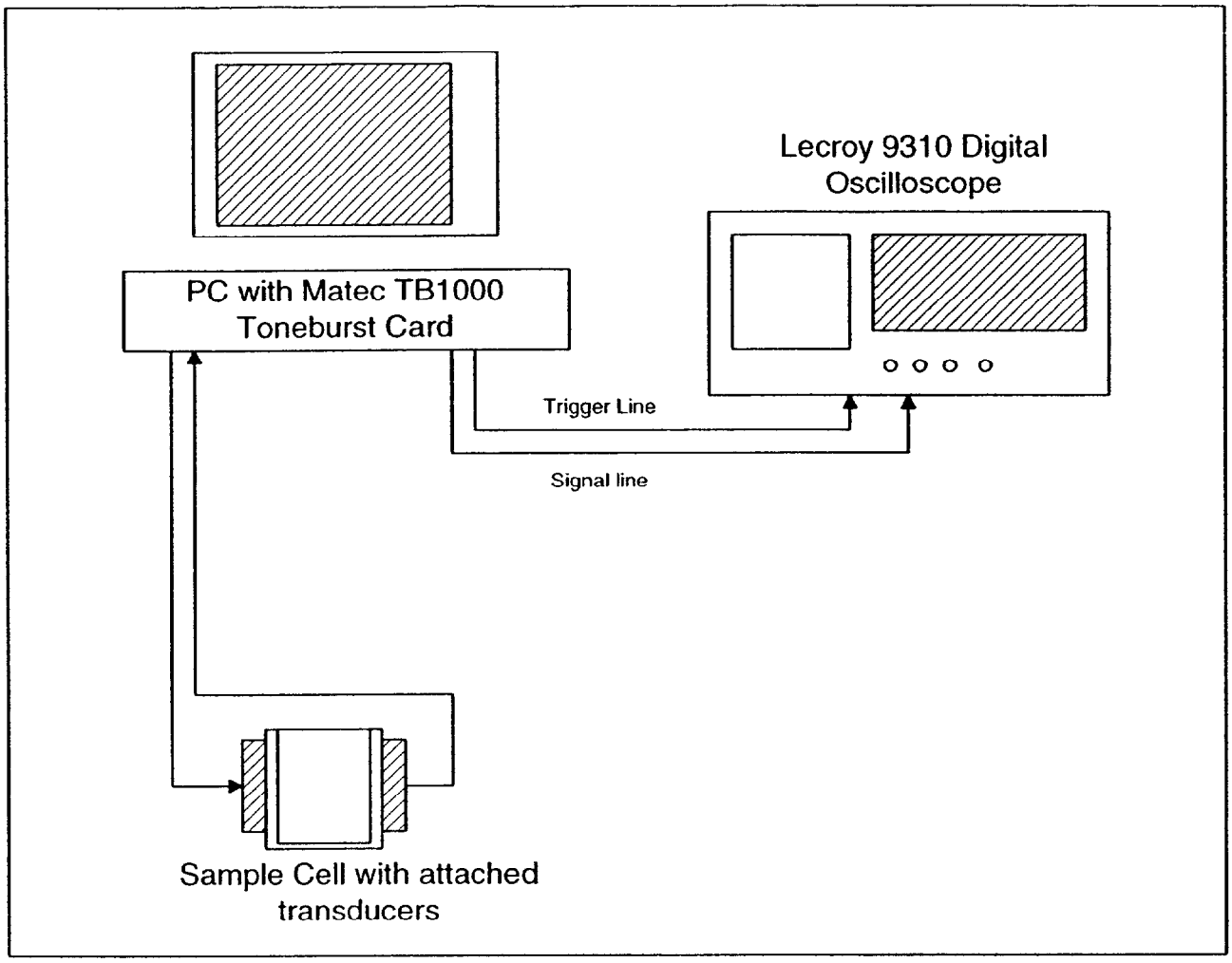

Figure 3.2: Schematic diagram of toneburst setup used to measure attenuation. A toneburst card located in a PC generates an electrical signal of constant frequency and transmits that signal to the transmitting transducer which is in contact with the sample. After traveling through the sample and being acquired by the receiving transducer the pulse is routed through the toneburst card to the oscilloscope.

measurements. It was found that 50 sweeps produced an acceptable average waveform with little noise, and had a short enough sampling time (~2 seconds) that settling of the slurry was insignificant. This finding is reinforced using Stokes law - under average experimental conditions terminal settling velocity is 3.4×10^{-4} m/s, giving a 6.7×10^{-2} cm drop during the two second sampling period.

As mentioned above, the spike pulse / FFT was found to be the preferred method for measuring attenuation. It was found to be much more accurate and consistent. The data it produces have much less noise than data resulting from the toneburst method. This is mainly due to the fact that only 2 experiments need to be performed using the pulse/FFT method (sample and reference) per pair of transducers, while up to 60 experiments per pair of transducers would be needed using the toneburst method to cover the same range and resolution. Nevertheless, both methods were employed to prove the consistency of the spike pulse/FFT.

The transducers used were immersion transducers made by Panametrics. Like a speaker, a specific transducer can only create/read ultrasonic signals in a specific frequency range. In order to cover the entire range desired (0.5 to 13 mHz), different transducers with different center-line frequencies must be employed. Five different pairs of transducers were used in this study, with centerline frequencies of 1 mHz, 2.25 mHz, 5 mHz, 7.5 mHz, and 10 mHz. See Appendix III for the frequency range, model number and serial number of all transducers used.

The test cell used for all attenuation experiments was a Plexiglas vessel with a nominal pathlength of two inches. The two inch pathlength was chosen because 2 inches is the diameter of the pipe used to transfer slurries at Hanford. The cell used can

accommodate transducer pairs with centerline frequencies of 1 MHz to 10 MHz. See Figure 3.3 for the schematic of the cell.

3.2 ATTENUATION EXPERIMENTS

3.2.1 SODA LIME GLASS

The first system studied is soda-lime glass beads in distilled water. Volume fraction ranged from 0.004 to 0.05. The particles, supplied by Cataphote® , Inc., have an average radius of 32 μm, and standard deviation of 7.6 μm. Particle density is 2.54 g/cm^3. See Table 3.1 for further information on physical properties.

	Soda-lime Glass	Water
Density (g/cm^3)	2.54	1.0
Thermal Conductivity (J/K·cm·s)	9.6×10^{-3}	5.87×10^{-3}
Specific Heat (J/g·K)	0.836	4.19
Thermal Expansion Coefficient (K^{-1})	3.2×10^{-6}	2.04×10^{-4}
Attenuation Coefficient per f^2 (s^2/cm)	1.0×10^{-15}	2.5×10^{-16}
Sound Speed (cm/s)	5.2×10^{5}	1.48×10^{5}
Shear Viscosity (g/cm·s^2)	-	1.01×10^{-2}
Shear Rigidity (g/cm·s^2)	2.8×10^{11}	-

Table 3.1: Physical properties of Soda-lime glass / water system. Properties are from Kinsler et al. (1982) and Bolz (1973)

Slurries were prepared by weighing a calculated amount of solids into a disposable beaker and then adding the correct amount of water. Volume fraction Φ was determined by:

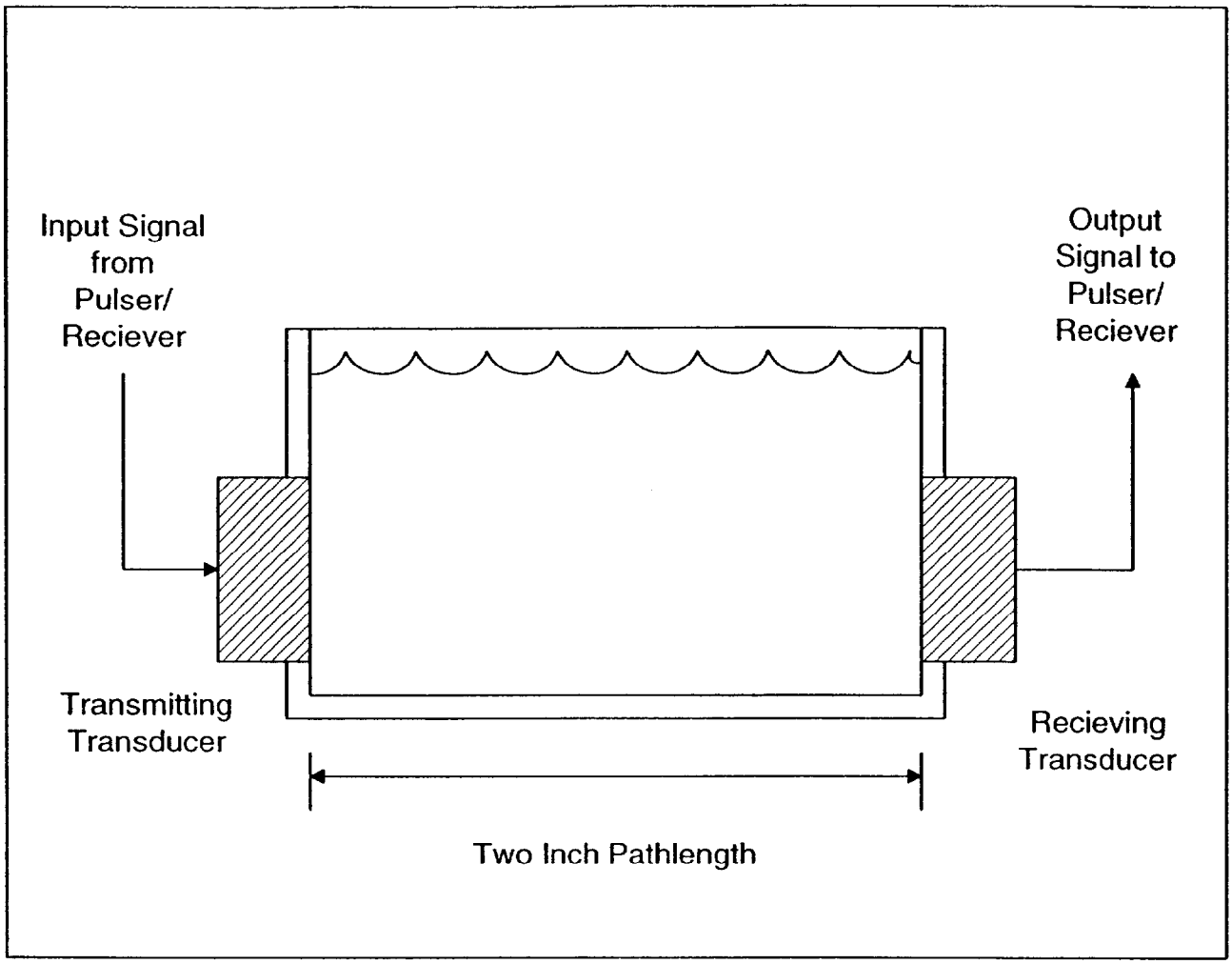

Figure 3.3: Schematic diagram of attenuation test cell. Cell is constructed of Plexiglas with a nominal pathlength of two inches. Transducers with centerline frequencies of 1 MHz to 10 MHz are mounted on each side to complete the cell.

$$\Phi = \frac{volume_{solids}}{volume_{solids} + volume_{liquid}} = \frac{\frac{g_{solids}}{\rho_{solids}}}{\frac{g_{solids}}{\rho_{solids}} + \frac{g_{liquid}}{\rho_{liquid}}} \qquad (2)$$

where

g_{solids} = mass of solid particles added (g)
g_{liquid} = mass of suspending liquid added (g)
ρ_{solid} = density of solid particles (g/cm^3)
ρ_{liquid} = density of suspending liquid (g/cm^3)

Slurries were prepared immediately prior to testing. The test cell was prepared with the appropriate transducers, and the pathlength measured using a dial caliper. The sample was hand stirred with a stainless steel spatula and a reading was taken.

In order to determine the best frequency range for studying low Φ slurries, a sample was interrogated with all 5 pairs of transducers. In addition, both the pulse/FFT and toneburst methods were employed.

The standard method of obtaining a baseline reading had been to fill the cell with water, take a reading, and empty and dry the cell. Slurry would then be added to the cell to collect the sample reading. This method had several disadvantages - it was time consuming and it introduced more possibilities for error. For example, the handling of the cell necessary to empty, dry, and refill it could cause the pathlength to change slightly. In addition, the time lapse between gathering the two signals could lead to slight changes in the waveform produced by the pulser/receiver or toneburst card. The attenuation calculation is based on the assumption that the slurry and the suspending liquid are both subjected to the same waveform. Any change in that waveform could lead to error.

Without stirring, the soda-lime glass beads settle to the bottom of the vessel quickly. This behavior was exploited to improve the method of determining the water signal. Since only a small amount of solids was used for these experiments, after they settled the space between the transducers contained only distilled water. Therefore, the completely settled system was used to acquire the baseline reading. Immediately after the baseline reading was taken, the system was stirred until all solids were resuspended and the sample reading was taken.

3.2.2 CLAY SURROGATE

After preliminary work with soda lime glass at low Φ it was decided to attempt to use ultrasound to characterize a system more representative of the nuclear waste. A number of surrogate slurries have been developed to simulate nuclear waste (Golcar 2000), one being a primarily rhealogical surrogate composed of bentonite and kaolin clays. The slurry selected for these experiments consisted of two parts (dry weight) kaolin to one part bentonite.

Kaolin clay is composed mostly of silica and alumina arranged in alternating layers. A particle is generally square shaped, with sides less then 1-2 μm in length. The particles, held together by strong hydrogen bonds, can be 70 to 100 layers thick. (Holtz and Kovacs, 1981) Bentonite is actually a mixture of several different types of minerals, with smectite as the major component (Grim 1968).

Since Bentonite particles swell when added to water it is important to prepare the slurries some time before testing. A Lighnin® mixer was used to provide the high shear that is needed to properly disperse clay. Kaolin was added to water and the mixture was

stirred until the clay was dispersed (usually about 15 minutes). Then bentonite was added and the mixture was stirred again. The slurries were allowed to sit overnight and then mixed again before testing.

The test procedure was similar to that performed on the soda lime glass. Only one set of transducers (10 MHz) was used. The pulse/FFT method was the only testing method employed. Since lay does not settle readily, a baseline reading was acquired in distilled water. Since the density of the clay particles was not known slurries were prepared on a weight fraction basis, with weight fractions ranging from one to five percent.

3.2.3 CRYSTALLIZED SALT SOLUTION

The third system studied is a crystallized salt solution proposed by researchers at the Hanford site to represent the chemical and physical behavior of an average composition of Hanford supernate nuclear waste containing suspended saltcake particles, with the exception of the radioactive properties. All of the major components in the waste tanks are present in the chemical slurry surrogate, and they are in the correct proportions. See Table 3.2 for the chemical species present, and the concentration of each species:

Chemical Species	Feed Solution (M)	Concentrated Solution (M)	Weight Percent
NaOH	1.61	2.3	5.9
$NaAl(OH)_4$	1.54	2.2	16.3
$NaNO_3$	2.59	3.7	20.3
$NaNO_2$	2.24	3.2	14.3
Na_2CO_3	0.42	0.6	4.1
H_2O			31.7

Table 3.2: Crystallized Salt Solution components

In brief, the solution is prepared by dissolving all of the solids in water and then evaporating the solution down to 70% of the original volume to form a precipitate. The complete procedure is described in Appendix I. The mixture is centrifuged to separate the solids (precipitate) from the liquid (supernate). The solids are stored wet to prevent caking and the density of the supernate is measured.

Again, the procedure used to determine the attenuation of the surrogate slurry was similar to that used on the soda lime glass beads, except that only the 10 MHz transducers and the pulse/FFT method were employed. The baseline reading is acquired in supernate. Solids are added gradually with intermediate testing to get attenuation data at different weight fractions.

The actual volume (or weight) fraction studied is not known, since it is difficult to measure the density of the solids, and the solids are not dried out completely. Accordingly, the following procedure is employed to estimate the weight percent solids in the slurry. Assuming a packing efficiency of 60% and a solid density of 2.2 gm/cm^3 (typical of sodium salts, according to Weast, 1972) an approximate dry weight percent of the concentrated solids feedstock is given by:

$$W_{dry} = W_{wet} \times \frac{1cm^3}{1.91g} \times 0.6 \times \frac{2.2g}{cm^3} \qquad (3)$$

where:

0.6 = Assumed packing efficiency (volume fraction of concentrated solids)
2.2 g/cm3 = Assumed dry solids density
1.91 g/cm3 = Assumed density of wet solids

3.3 SPEED BACKGROUND

Previous work (Norato 1999) characterizing slurries using ultrasound had dealt with measuring attenuation exclusively. Theory was developed (Spelt et al., 2000) that predicted ultrasonic speed. In order to test the theory and evaluate the utility of speed information in characterizing slurries it was deemed desirable to develop a method to measure ultrasonic speed as a function of frequency in liquid slurries. The technique developed by McClements and co-workers (1991) was selected because it is proven successful and is similar to the method already in use to measure attenuation

The technique uses a dual reflectance method, along with an FFT, to measure sound speed. The experimental setup, shown in Figure 3.4, is very similar to the Spike Pulse/FFT setup used to measure attenuation. The test cell, as depicted in Figure 3.5, is similar to that used to measure attenuation, but only one transducer is used. Instead of being in direct contact with the fluid, the transducer is in contact with a Plexiglas buffer. Ultrasound gel (Parker Laboratories Scan gel) is used to couple the transducer to the Plexiglas. The sample is on the other side of the Plexiglas buffer. A brass reflector plate is mounted on the rear of the cell. The reflector plate is constructed of brass due to its high impedance and its resistance to corrosion. The reflector is removable and the pathlength can be altered by installing a thicker or thinner reflector plate. For these experiments two reflector plates were used, a thinner one that gives a pathlength of one inch, and a thicker one that gives a pathlength of ½ inch.

A spike pulse waveform is used to energize the transducer. As the sound travels through the cell it is actually reflected twice - once at the Plexiglas/sample interface and

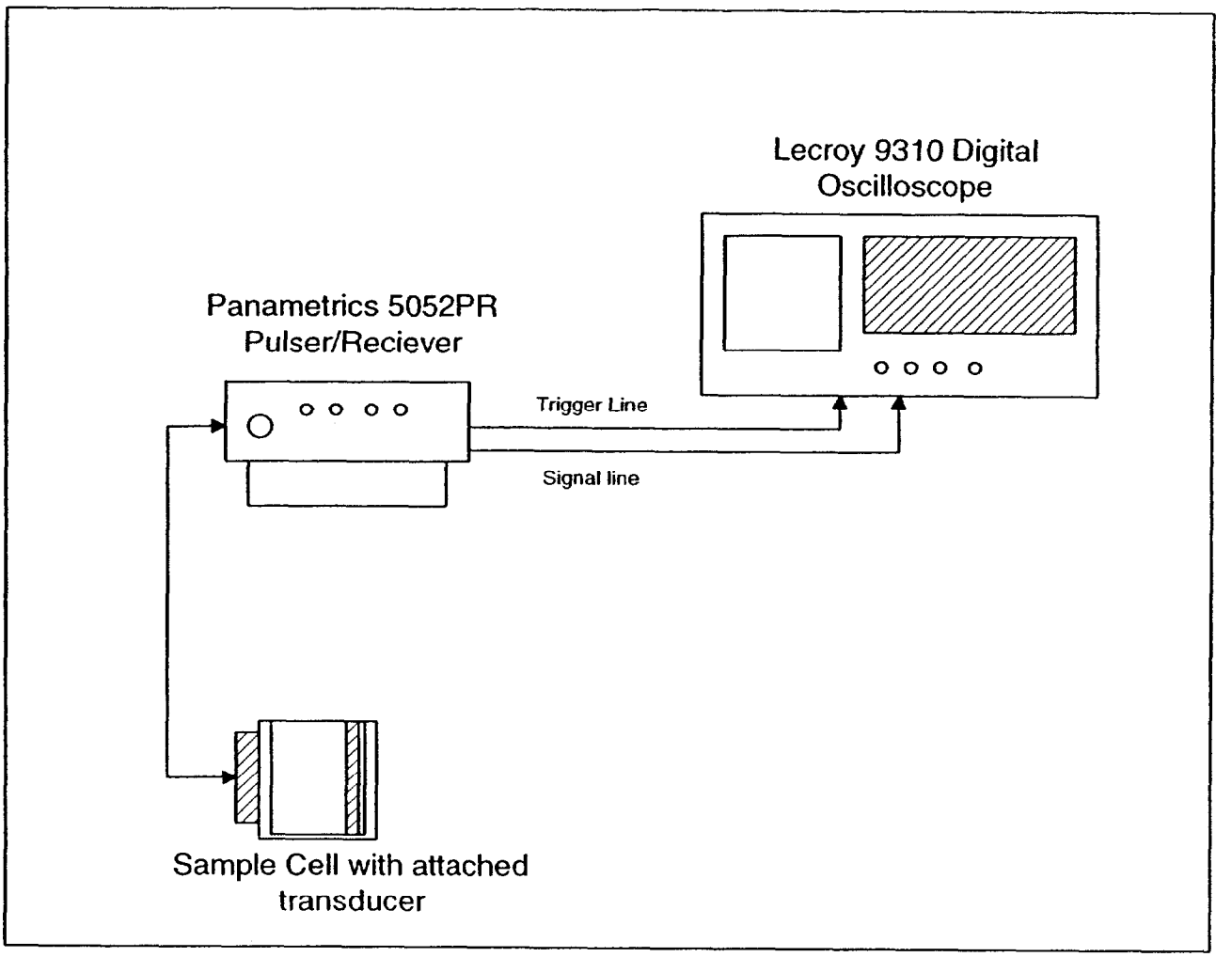

Figure 3.4: Schematic diagram of setup used to measure speed. A spike pulse is generated by the pulser/receiver and is transmitted to the transducer, which is coupled to a Plexiglas® buffer with ultrasound gel. The signal travels through the buffer and some signal is reflected back at the buffer/sample interface. The remaining signal travels through the sample and is reflected off a brass plate mounted at the far end of the cell. The same transducer that emitted the signal picks up both reflections and routes the reflected signals through the Pulser/Receiver to the oscilloscope.

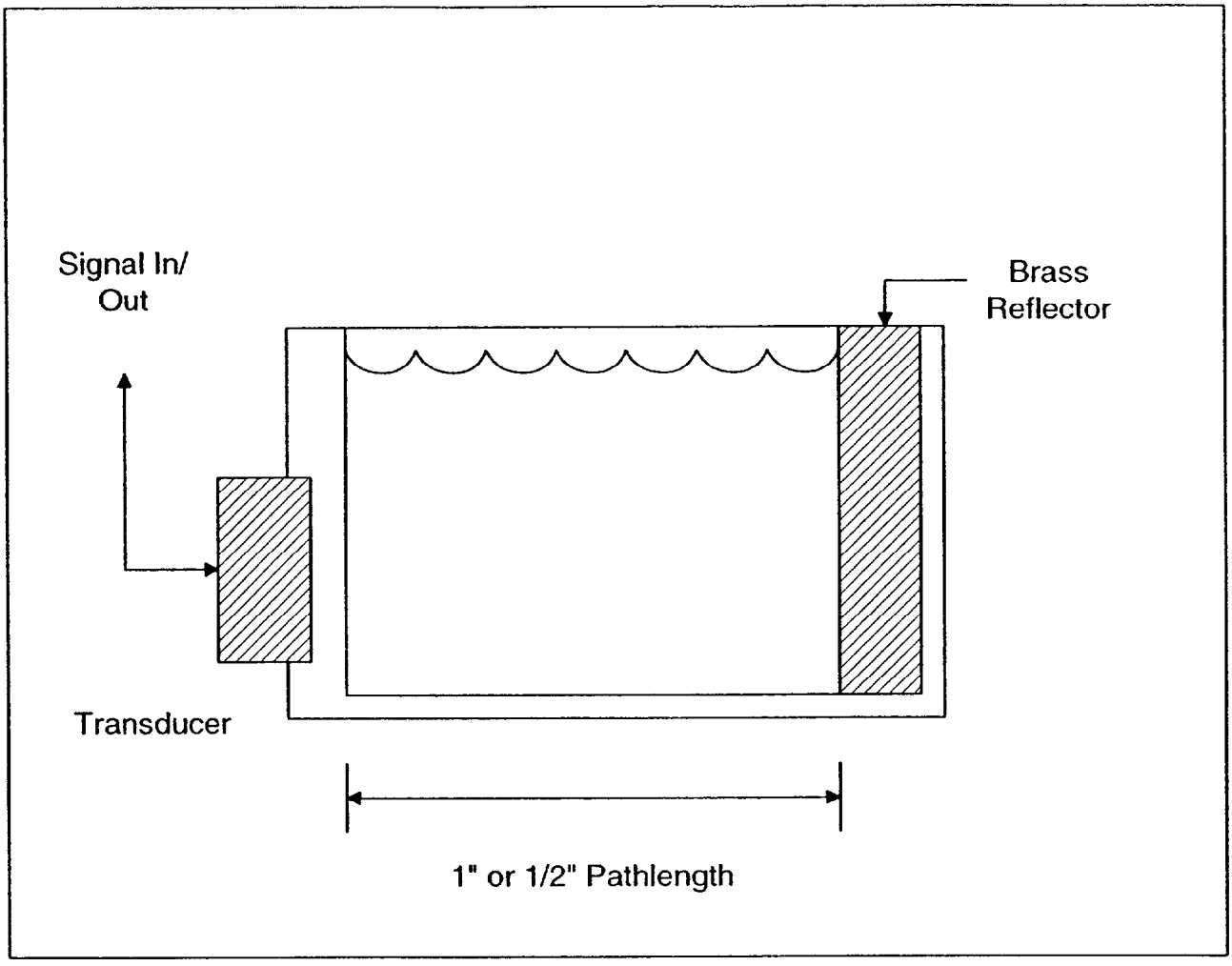

Figure 3.5: Schematic diagram of speed test cell. Cell is constructed of Plexiglas with a brass reflector plate. The reflector plate is interchangeable, with current plates creating pathlengths of ½ inch or one inch. A single transducer is mounted on one side, coupled with ultrasound gel. The signal passes through a buffer rod of Plexiglas (thickness: ¼ inch) before coming in contact with the sample.

again off the brass reflector at the far end of the cell. See Figure 3.6 for a typical waveform produced by this setup. Since travel time through the wires, transducers, Plexiglas buffer, and other electrical components is common to both signals the exact travel time through the sample can be calculated by subtracting the time of the first peak from the time of the second peak. As shown below, by using an FFT to calculate the phase difference between the two reflected signals the speed as a function of frequency can be measured.

The test cell must be designed properly in order to produce acceptable data. The Plexiglas buffer must be thick enough such that the transducer stops ringing before the first reflection reaches it. Plexiglas, like all materials, absorbs sound, and so if the buffer is too thick the signal will be attenuated and signal will be lost unnecessarily. In addition, the buffer thickness and sample pathlength must be designed so that signals which reflect internally in the buffer rod do not interfere with the second echo returning from the brass reflector.

The phase speed is calculated using the following equation (McClements, 1991):

$$c = pathlength \times \frac{360 \cdot f}{(n \cdot 360 + \delta\theta - \theta_d - 180)} \qquad (4)$$

where

c = phase speed
f = frequency
$\delta\theta$ = phase difference from FFT
θ_d = phase correction due do diffraction (usually negligible)
n = number of waves ~ $\Delta t * f$
and Δt (above) = time difference between main peaks of the two reflections

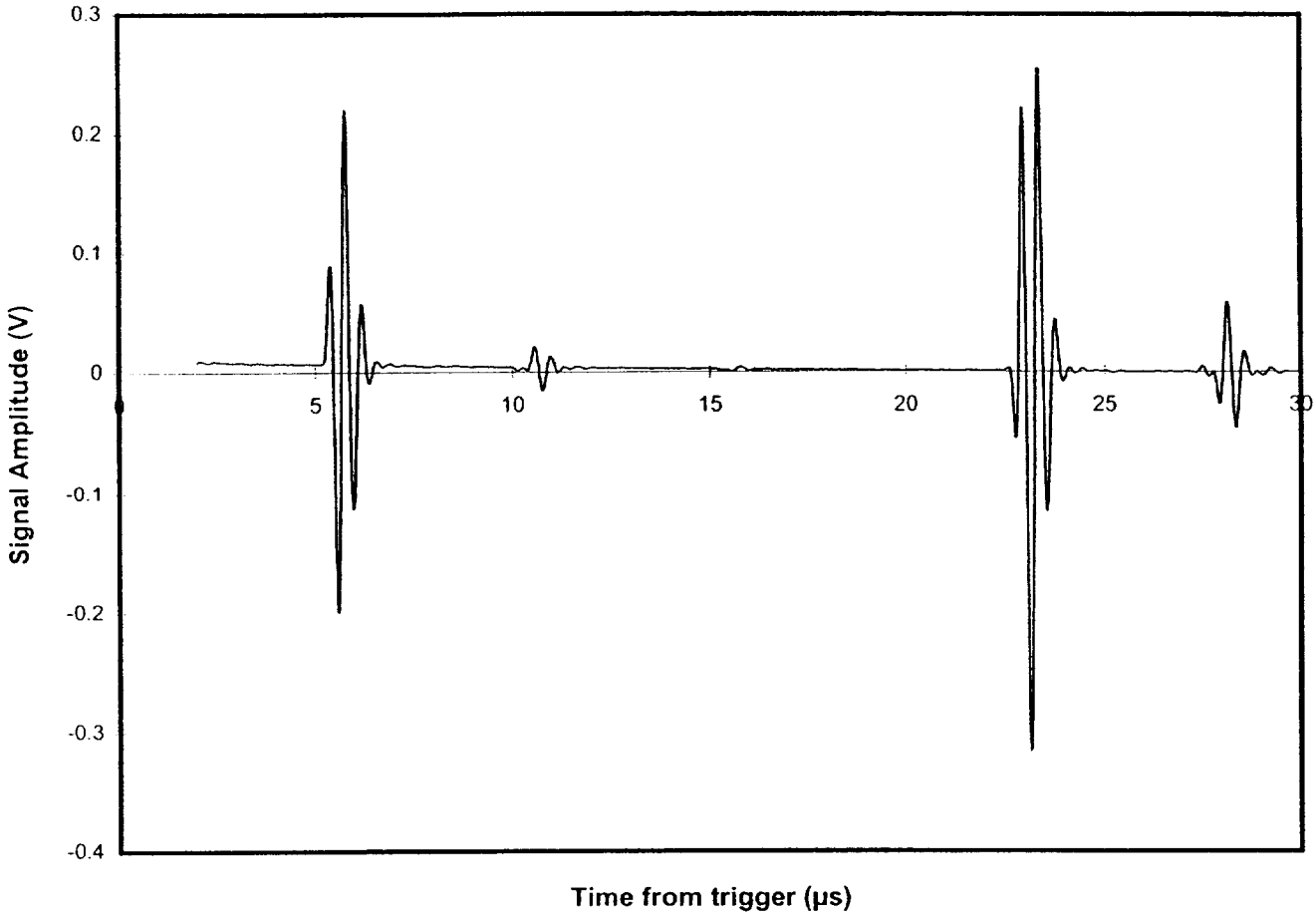

Figure 3.6: Typical waveform produced from speed test setup. The first peak, at t~6 μs, is reflected at the buffer-rod sample interface. The second peak, at t~23 μs, is reflected off the brass plate at the far end of the cell. The smaller peaks at t ~11 μs and t~28 μs are echoes of the larger peaks.

The main peaks of the two waveforms are superimposed and a phase FFT operation is performed on both. The difference in phase between the first and second echo as a function of frequency is determined. The 180 degree correction is required because the signal is inverted as it reflects off the brass plate. In practice, it was easier to superimpose the waveforms if the second echo is inverted employing software available with the oscilloscope. Accordingly, the 180 degree correction was not necessary.

The speed of sound in water is strongly dependent on temperature. At room temperature the speed of sound increases approximately 3 m/s for every degree Celsius the temperature is increased. Although this change is small compared to the speed of sound in water at room temperature (~1500 m/s at 23 °C) it has a significant effect when trying to correctly discern the volume fraction of suspended particles. In order to provide better temperature control the test cell (with attached immersion transducer) is placed in a water bath (Neslab GP-300). Slurry temperature was maintained at 25 °C ±0.1°, verified by a digital thermometer (Cole-Parmer Thermistor Model 8502-12).

3.3.1 SPEED EXPERIMENTS

Speed measurements are made in a system consisting of the same soda-lime glass beads described above that were used for attenuation. In order to gauge the effect of particle size on speed larger particles, manufactured by Potter's Industries (P-0060, lot 0422(98)) are also tested. These particles are larger than those previously studied, with a mean diameter of 125 μm and a standard deviation of 19 μm. Although larger than the soda-lime glass beads the Potter's beads are composed of the same material (silica) so

physical properties for the Potter's beads were taken to be the same as those for soda-lime glass.

In order to accurately measure the speed of sound the pathlength must be known very precisely. For a ½ inch pathlength, a measurement error of 1/1000 of an inch results in an error of 3 m/s under typical conditions. In order to be able to measure the absolute sound speed with as little error as possible it is necessary to measure the pathlength to the 1/10,000 of an inch. Since it is impossible to measure this accurately in a direct fashion, the cell is calibrated using distilled water. The cell is filled with water and the transit time was measured at different temperatures. The speed of sound in water is very accurately known (Lynnworth) so with careful monitoring of temperature the pathlength can be calculated to the desired accuracy of 1/10,000 of an inch.

The speed of sound is measured in slurries of both the soda-lime glass particles and Potters' beads suspended in distilled water. Volume fraction ranges from 5% to 45%. Initially all 5 transducers were used, to cover the entire available frequency range, but for most experiments the 2.25 MHz transducer provided all the data necessary.

Experiments are also conducted at low volume fraction. Speed is measured in soda-lime glass slurries, at volume fractions of 0.004, 0.01, 0.03, and 0.05. For these experiments a "settled solids" approach similar to that used to measure attenuation is used. Speed is measured in distilled water, with the solids settled. Then the system is stirred to resuspend the solids, and the speed in the slurry is measured. The difference between the two velocities is calculated.

4. Theory

The theory used to predict attenuation in solid-liquid two phase systems is given in Spelt et Al. (2000). It uses an effective medium approach to predict viscous, thermal, and scattering losses. In this approach the particle is surrounded by a spherical shell of fluid. This particle-cell combination is immersed in a uniform suspension (the effective medium). The properties of the effective medium are determined by solving the governing equations for the particle-cell combination so they are consistent with the averaged equations for the suspension.

The theory in its entirety is very complex and will not be discussed here. A brief summary valid for dilute slurries, where one only has to consider the affects of a sound wave on a single particle will be given.

Epstein and Carhart (1953) first derived the wave equations for the interior and exterior of solid particles. They linearized the equations conserving mass, momentum, and energy, and eliminated pressure and internal energy using the linearized equations of state to give relationships in terms of speed, density, and temperature. The speed vector v can be expressed in terms of the vector potential A and a scalar potential ϕ as shown:

$$v = -\nabla\phi + \nabla \times A \qquad (1)$$

with $\nabla \cdot A = 0$. It is then possible to eliminate temperature and density to give a forth-order partial differential equation for ϕ and a second order equation in A. The ϕ expression can be split into two second order wave equations by substituting

$\phi = \phi_c + \phi_T$, with ϕ_c and ϕ_T being the scalar potentials of the compressional and thermal waves. The result is three wave equations:

$$\left(\nabla^2 + k_c^2\right)\phi_c = 0 \tag{2}$$

$$\left(\nabla^2 + k_T^2\right)\phi_T = 0 \tag{3}$$

$$\left(\nabla^2 + k_s^2\right)A = 0 \tag{4}$$

The wavenumbers in the above equations are given by

$$\frac{1}{k_c^2} = \frac{c^2}{2\omega^2}\left[1 - i(e+\gamma f) + \left\{\left(1 - i(e+\gamma f)\right)^2 + 4f(i+\gamma e)\right\}^{1/2}\right] \tag{5}$$

$$\frac{1}{k_T^2} = \frac{c^2}{2\omega^2}\left[1 - i(e+\gamma f) - \left\{\left(1 - i(e+\gamma f)\right)^2 + 4f(i+\gamma e)\right\}^{1/2}\right] \tag{6}$$

$$k_s = (1+i)\left(\frac{\omega\rho}{2\mu}\right)^{1/2} \tag{7}$$

with

$$e \equiv \left(\frac{4\mu}{3} + \kappa\right)\frac{\omega}{\rho c^2}; f \equiv \frac{\sigma\omega}{c^2} \tag{8}$$

In these expressions c is the phase speed in the pure liquid, ρ is density, κ and μ the compressional and dynamic viscosities, γ the ratio of specific heats (C_p/C_v), τ the thermal conductivity, and $\sigma = \tau/\rho C_p$ the thermal diffusivity.

Similar equations are valid inside the particles, with the dynamic viscosity replaced by $\tilde{\mu}/(-i\varpi)$ and the wave speed by $\left(\left(\tilde{\lambda}+2\tilde{\mu}/3\right)/\tilde{\rho}\right)^{1/2}$, where $\tilde{\lambda}$ and $\tilde{\mu}$ are the Lamé constants. The compressional viscosity of the solid is set to zero. The tilde notation refers to quantities inside the particles.

At small values of e and f (as in water) the above expressions for k_C and k_T simplify to

$$k_c = \frac{\varpi}{c} + \frac{i}{2}\left[\left(\frac{4}{3}\mu + \kappa\right)\frac{1}{\rho} + (\gamma - 1)\sigma\right]\frac{\varpi^2}{c^3} \qquad (9)$$

and

$$k_T = (1+i)(\varpi / 2\sigma)^{1/2} \qquad (10)$$

Equation (2) and its inside-particle counterpart represent the sound propagation through the slurry. The imaginary part of the wavenumber equals the attenuation. The bracketed term in equation. (9) is referred to as the 'diffusivity of sound'. The total attenuation coefficients in the liquid and in the solid particle will be treated as additional physical properties. The other two wave equations (3 and 4) describe waves due to thermal conduction and finite viscosity. Note that the modulus k_T in (10) is inversely proportional to the thermal penetration depth $\sqrt{\sigma/\varpi}$ and k_s is inversely proportional to the viscous penetration depth $\sqrt{\mu/\rho\varpi}$. Thermal (ϕ_T) and shear (**A**) waves usually have very high attenuation and are unimportant.

It is possible in principle to determine the phase speed and attenuation at arbitrary volume fractions using the above equations. The result can be determined by applying

boundary conditions of continuity to temperature, speed, heat flux and traction and solving the problem numerically.

The potential ϕ_c outside a particle located at $x_1$can be expressed as:

$$\phi_c(x) = \exp(ik_c \bullet x) + \sum_{n=0}^{\infty} i^n (2n+1) A_n h_n(k_c r) P_n(\mu) \qquad (11)$$

where $r = |x - x_1|$, $\mu = \cos\theta$, θ as the angle between $x\text{-}x_1$ and k_c. The spherical Bessel function of the third kind (or Hankel function) h_n corresponds to an outgoing scattered wave and P_n is the Legendre polynomial of degree n.

Inside the particle centered at x_1 we have

$$\langle \tilde{\phi}_c \rangle = \exp(ik_c) \sum_{n=0}^{\infty} i^n (2n+1) \tilde{A}_n j_n(\tilde{k}_c r) P_n(\mu) \qquad (12)$$

where j_n is the spherical Bessel function of the first kind. Similar expressions are written for ϕ_T and A. Expressions with a set of six unknowns for each mode n result. Application of the boundary conditions of continuity of speed, traction, temperature, and heat flux give six equation with six unknowns for each n. In a few limiting cases it is possible to solve for the unknowns analytically. However, it is best to solve the equations numerically since it is desired to cover a large range of frequencies.

After the coefficients are determined, the attenuation can be calculated per unit length using the result given by Allegra and Hawley (1972) as:

$$\alpha = -\frac{3\phi}{2z^2 a} \sum_{n=0}^{\infty} (2n+1) \operatorname{Re} A_n \qquad (13)$$

When the total volume fraction is small the above method can be extended to account for a non-uniform particle size distribution by summing up the attenuation caused by each individual particle size present:

$$\alpha_{tot}(f) = -\sum_{a=0}^{\infty} \hat{\alpha}(f,a)\phi(a)da \qquad (14)$$

where $\hat{\alpha}(f,a)$ is the attenuation density and $\phi(a)da$ is the volume fraction of a particular size range between a and $a+da$. Equation (14) is the basis of the computer program provided by Dr. Peter Spelt (2000) used with his assistance to calculate theoretical attenuation in solid-liquid slurries.

5. Results

Experimental results for the three systems studied follow. Included are comparisons of experimental results with theory and a study evaluating the reproducibility of the experimental data.

5.1 ATTENUATION IN DILUTE SODA-LIME GLASS BEADS

Figure 5.1 shows attenuation versus volume fraction at three different frequencies - 8 MHz, 10 MHz, and 12 MHz, for dilute soda-lime glass beads in water. Volume fraction ranged from 0.04% to 5%. As expected the relationship between attenuation and volume fraction is linear, with R^2 ranging from 0.9853 to 0.9986. Note that attenuation is significant (and measurable) even at very low volume fractions. Figure 5.2 shows the data at extremely low volume fraction (less than 2%).

Figure 5.3 shows a typical attenuation versus frequency curve. Note the unexpected maximum at low frequencies. It is suspected that the particles are slightly

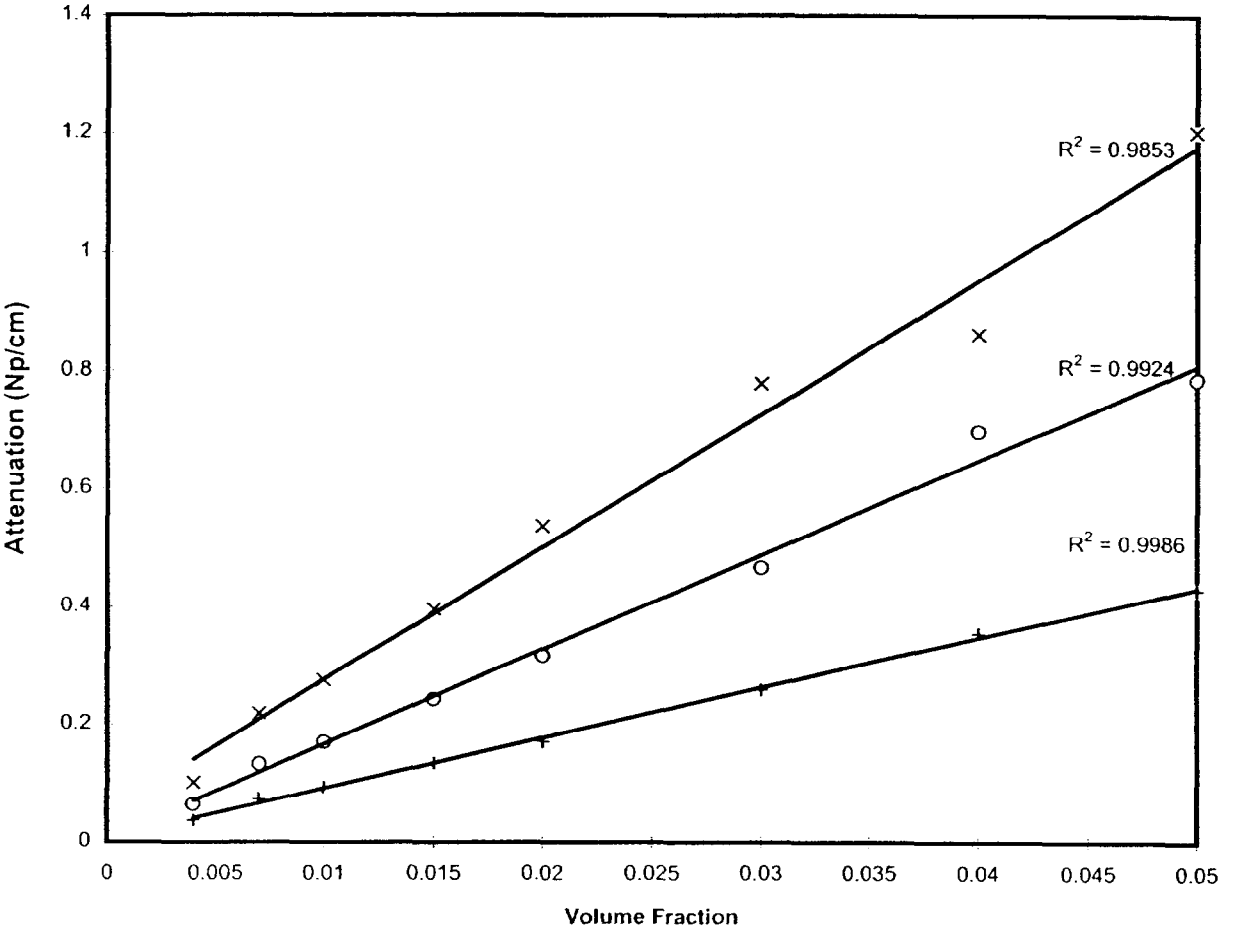

Figure 5.1: Attenuation versus volume fraction for a slurry of soda lime glass particles (radius=16 μm) in water at three frequencies. The frequencies studied are (×) 12 MHz, (o) 10 MHz, and (+) 8 MHz.

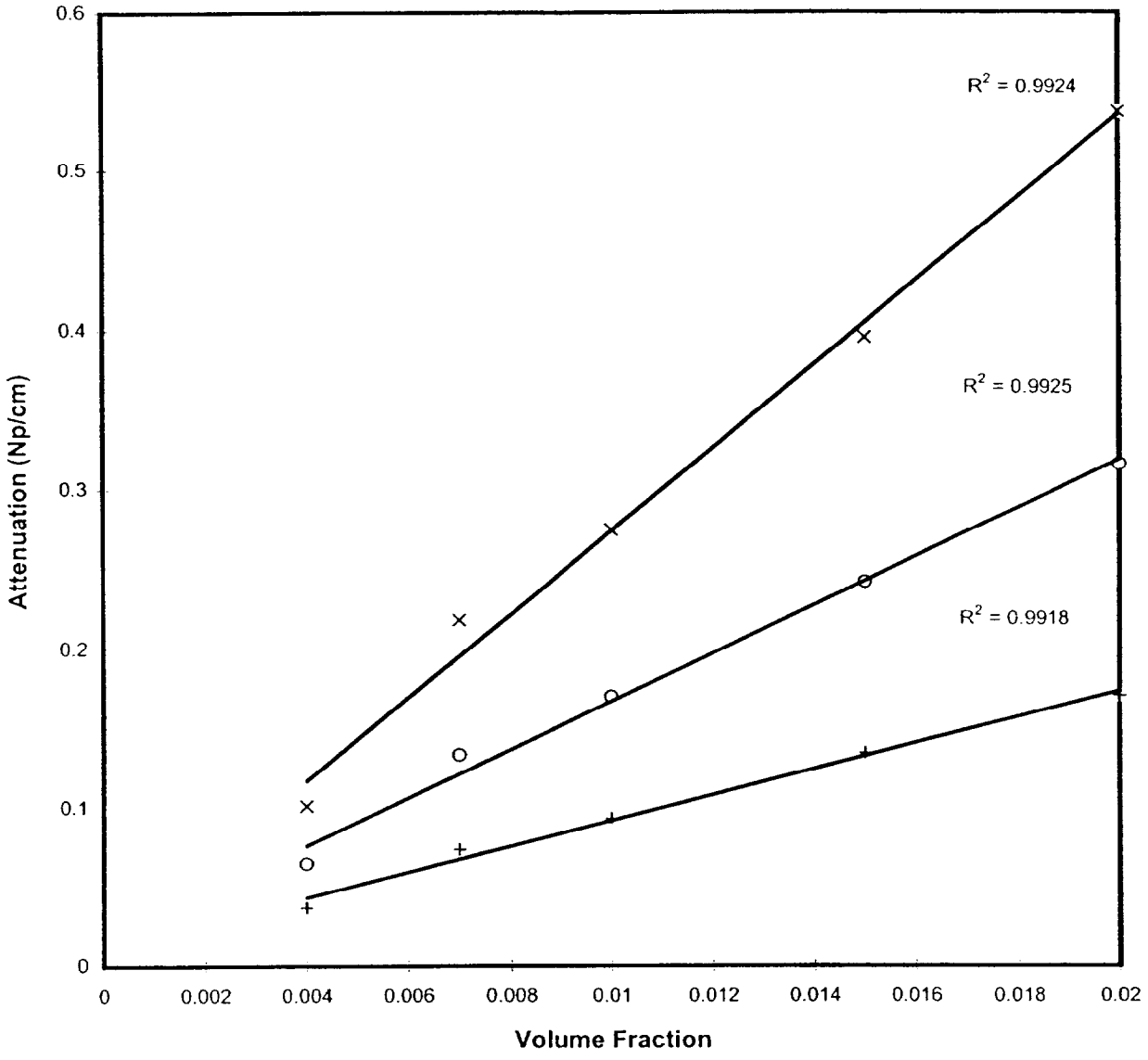

Figure 5.2: Attenuation versus volume fraction for a slurry of soda lime glass particles (radius=16 μm) at very low volume fraction. The frequencies studied are (×) 12 MHz, (o) 10 MHz, and (+) 8 MHz.

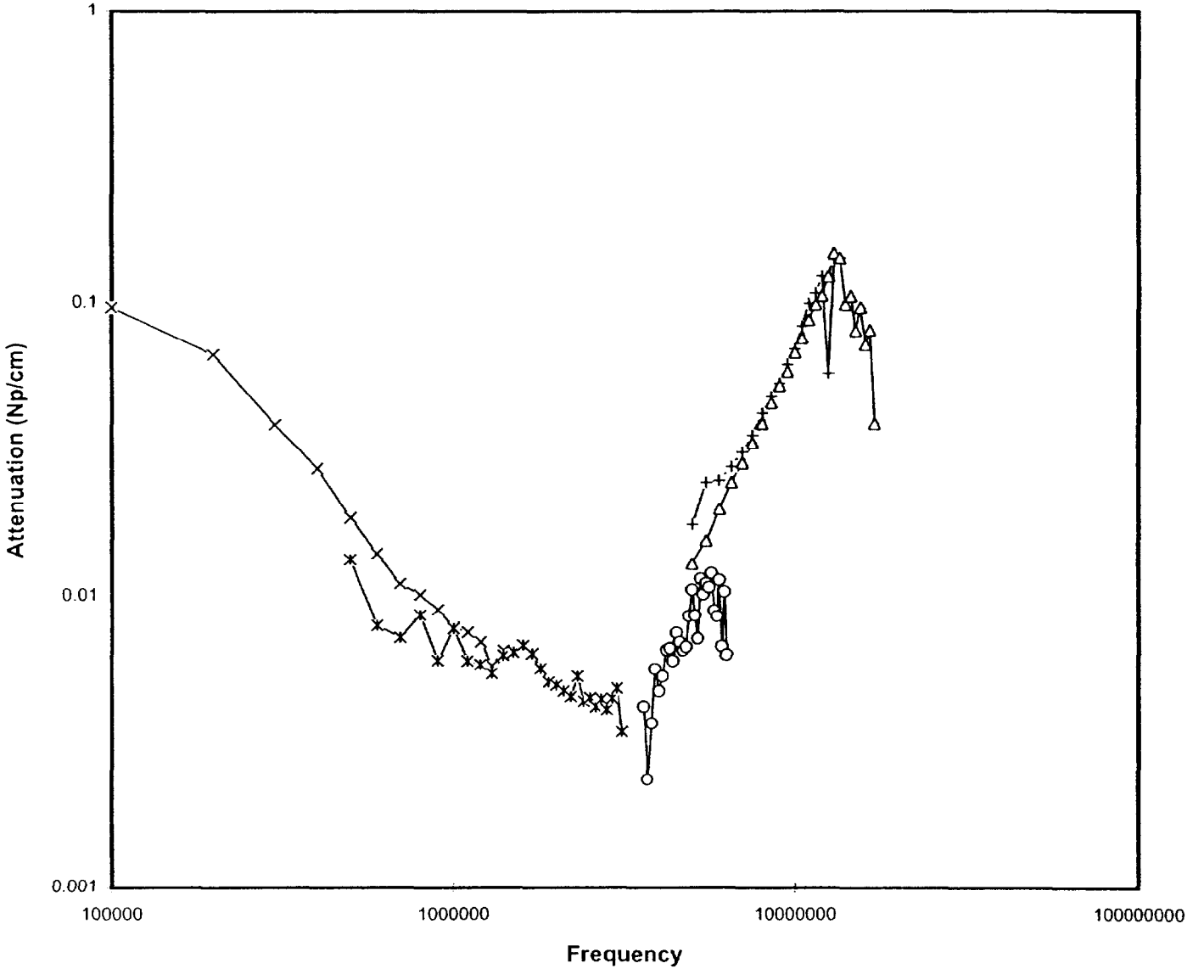

Figure 5.3: Typical attenuation versus frequency behavior for a 0.4% (volume) soda lime glass slurry. Transducers used are (×) 1 MHz, (*) 2.25 MHz, (o) 5 MHz, (+) 7.5 MHz, (Δ) 10 MHz.

porous, and this increase in attenuation is due to air entrained in the particles, as the behavior is similar to that observed when air bubbles were present in slurry (Norato 1999). In these experiments the slurry was tested immediately after preparation so there is no time for entrained air to diffuse out of the particles. In a subsequent experiment the slurry is prepared a week prior to testing, to allow time for any entrapped gas to diffuse out from within the porous particles and disengage. As shown in Figure 5.4, the low frequency attenuation decreased significantly. It was also noted that the attenuation at higher frequencies was essentially unchanged. Gas bubbles resonate at a specific frequency which is a function of the size of the bubble. At frequencies much higher than the resonance frequency the presence of gas bubbles has little effect on attenuation

As mentioned previously, several different methods are attempted in order to determine the best way to measure attenuation at low volume fraction. Figure 5.5 shows a comparison between the pulse/FFT method and the toneburst method. The pulse/FFT data are less noisy and are more consistent from transducer pair to transducer pair.

Figure 5.6 shows the difference between acquiring the baseline signal in the settled slurry and acquiring the baseline signal separately. The signal acquired using the pulse / FFT method is significantly less noisy.

5.1.1 COMPARISON WITH THEORY

As shown in Figure 5.7, the effective medium theory predicts the behavior of the system well. Attenuation varied linearly with volume fraction. The slight deviation present at lower frequencies may be caused in part by entrained air, as discussed previously.

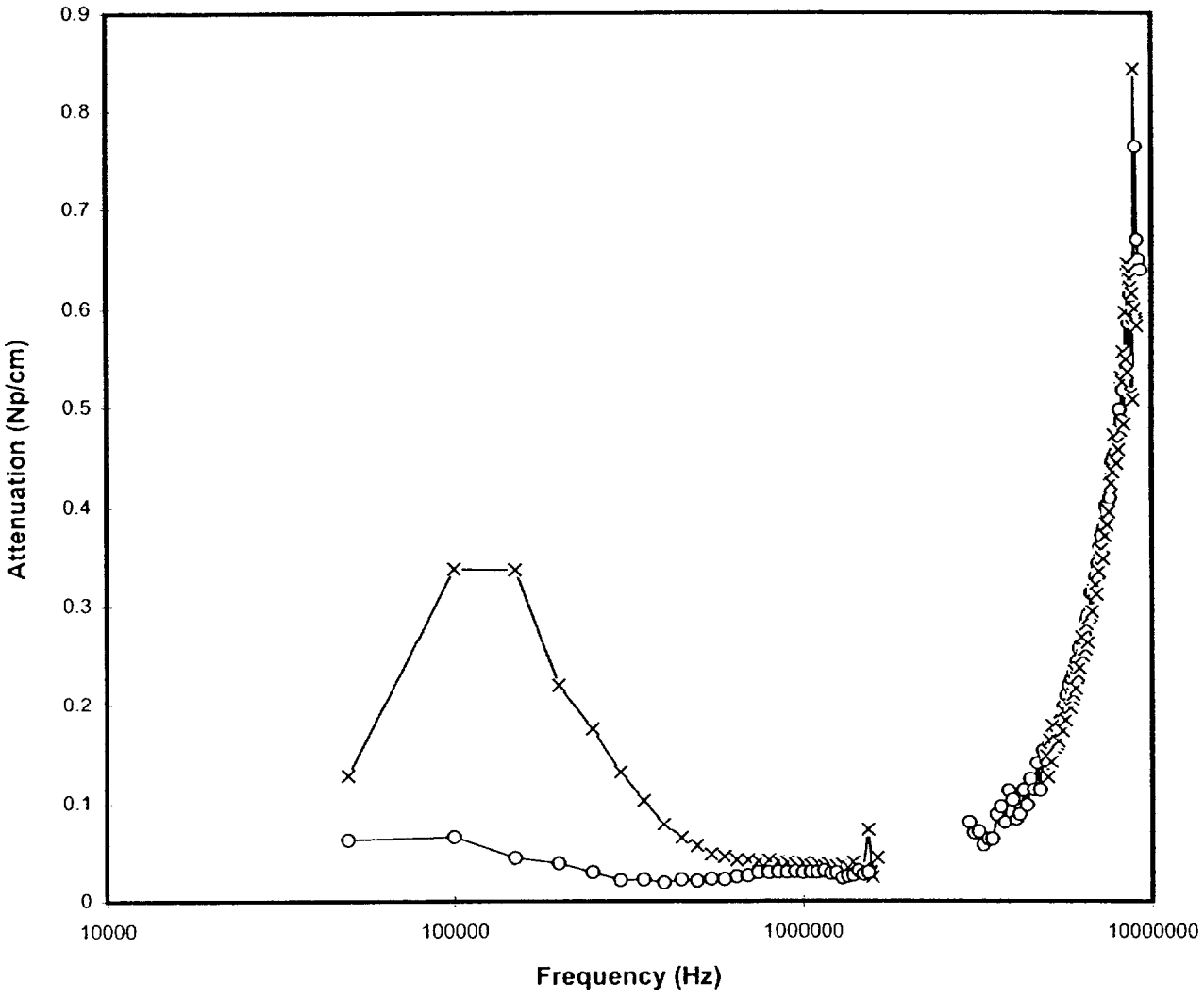

Figure 5.4: Effect of time between preparation and testing in soda lime glass slurries. The data marked (×) was collected immediately following preparation of the slurry. The data marked (o) was collected after that same slurry was allowed to sit one week.

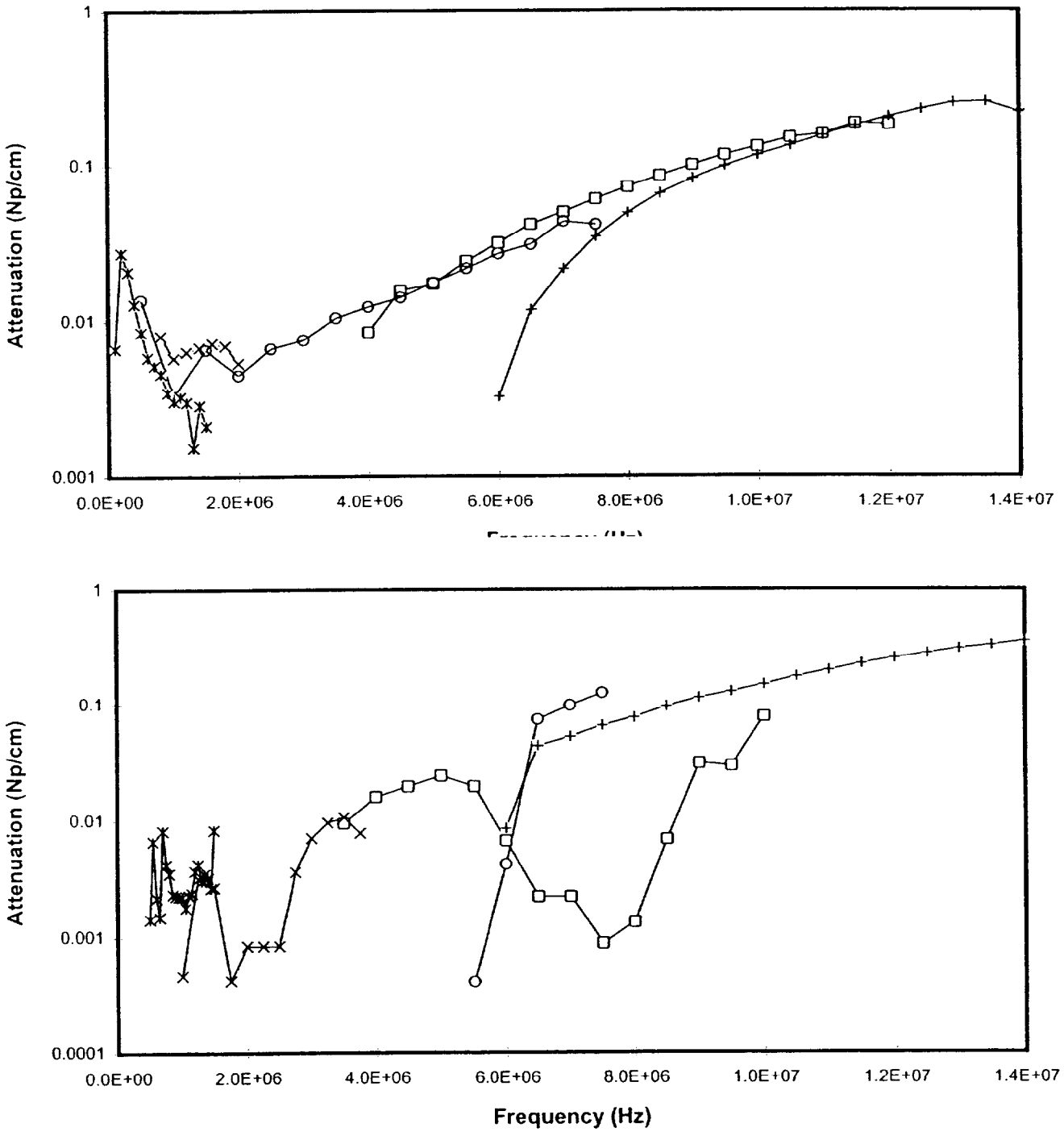

Figure 5.5: Comparison of pulse/FFT and toneburst methods of measuring attenuation. Pulse/FFT data is shown on top, with toneburst data shown on bottom.

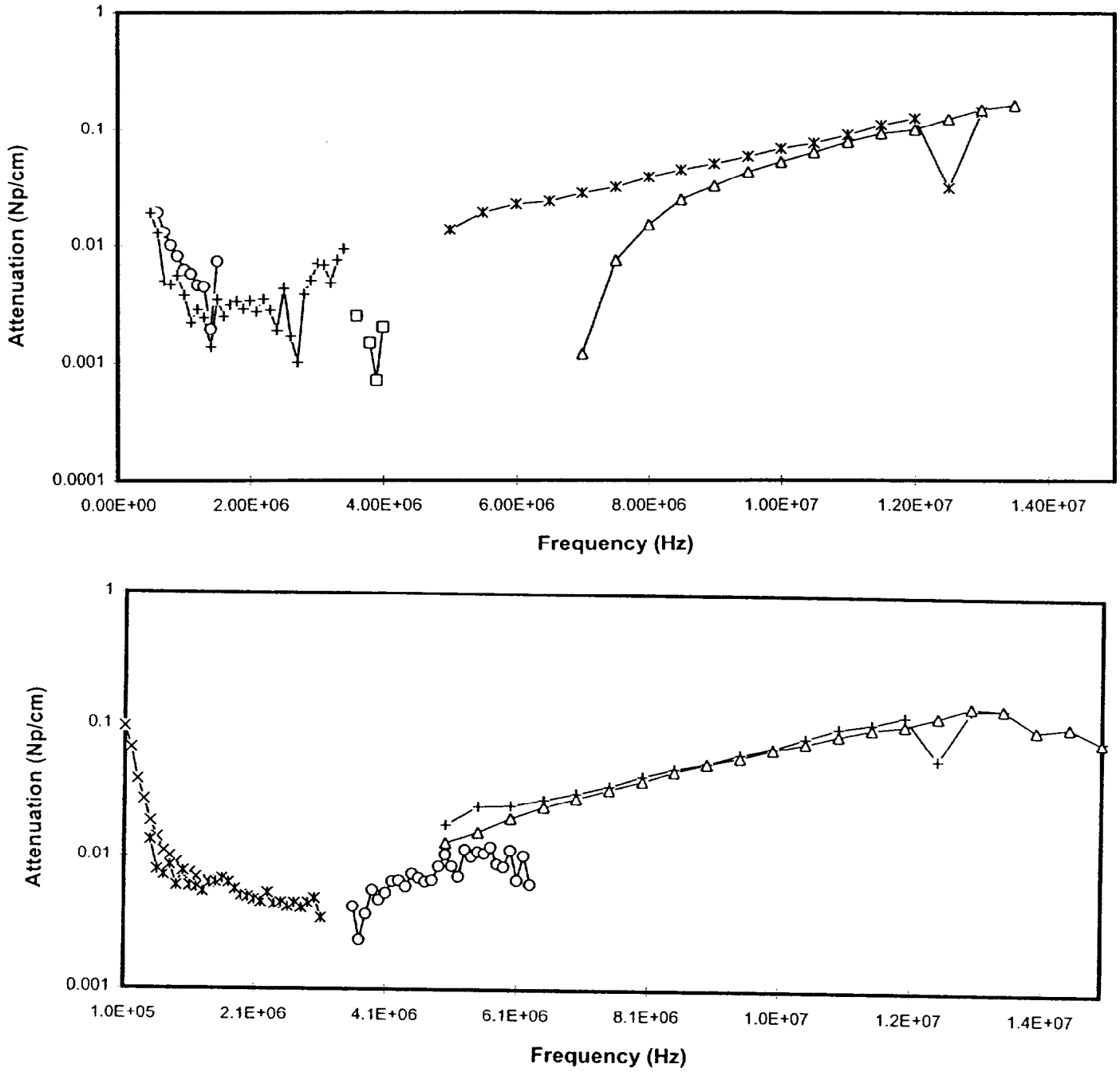

Figure 5.6: Comparison of methods of acquiring baseline signal. The baseline signal for the data shown on top was acquired separately from the sample signal. The baseline signal for the data shown on bottom was acquired by letting the solids settle.

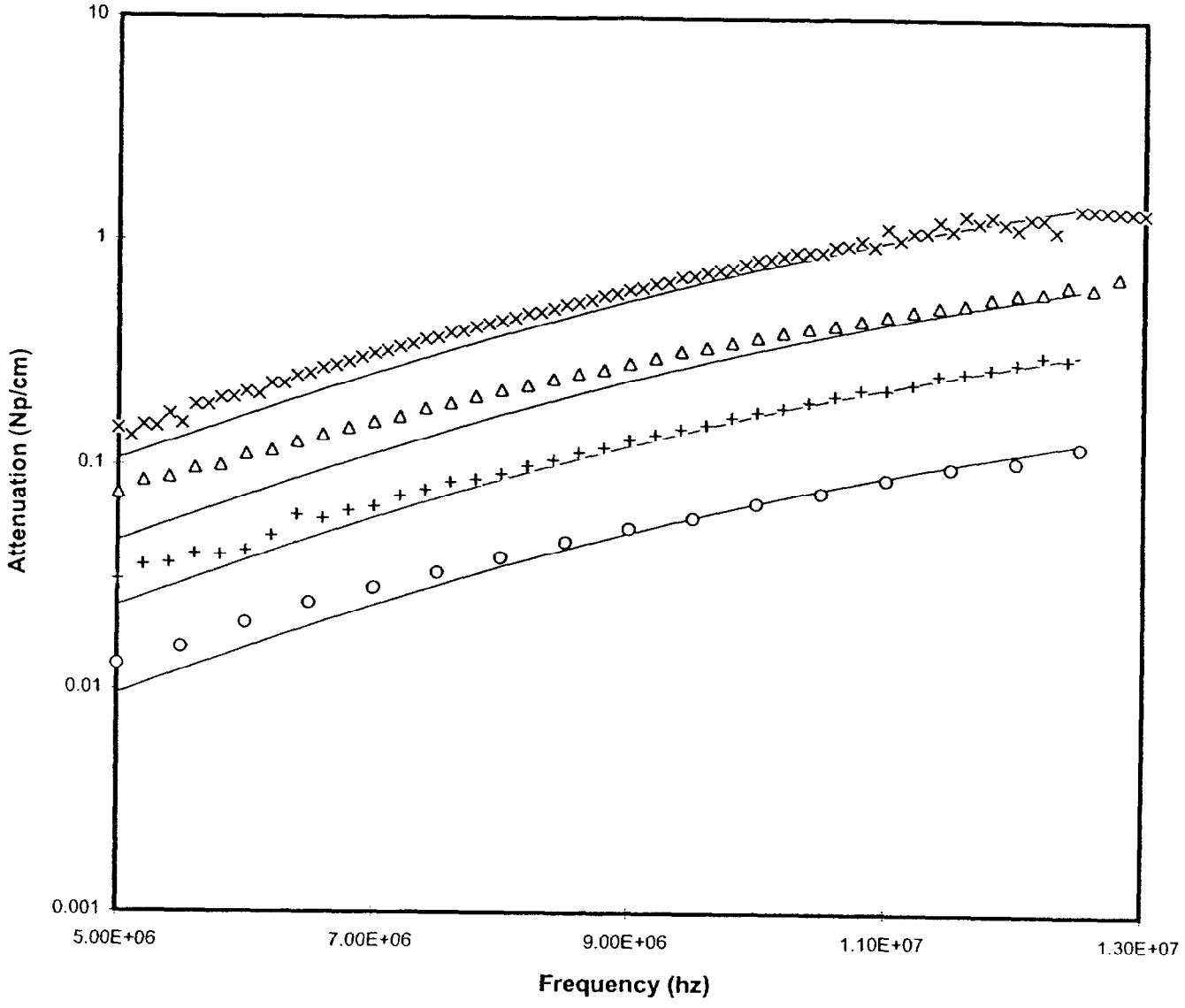

Figure 5.7: Comparison of theoretical prediction and experimental data of attenuation versus frequency for slurries of soda lime glass in water. The points represent experimental data and the lines represent theoretical predictions. The same pair of 10 MHz transducers was used to gather all data. Volume fractions shown are (o) 0.004, (+)0.01, (Δ) 0.02, and (×) 0.05.

5.2 ATTENUATION IN CLAY MIXTURES

Figure 5.8 displays attenuation versus volume fraction in the clay mixture system. Results are similar to those found in soda-lime glass. Attenuation is a linear function of volume fraction at constant frequency (R^2 ranges from 0.9997 to 0.9999), and increases with increasing frequency. There is less scatter with the BKC system than with the SLG system. This is probably due to the fact that clay does not settle easily and variations due to nonhomogeneity are much less.

Suprisingly, the linear fit does not pass through the origin, whereas the linear fit for the SLG system does. As mentioned before, clay particles swell in water and are not as rigid as solid particles such as soda-lime glass beads. The swelling may cause unexpected behavior such as that observed.

5.3 ATTENUATION IN CHEMICAL SURROGATE

Figure 5.9 displays attenuation as a function of weight fraction in the CSS system. The relationship is linear as expected. Also of interest is Figure 5.10, which displays attenuation as a function of frequency for ~1% (weight) chemical slurry surrogate. The relationship between attenuation and frequency also appears linear. The relationship between attenuation and frequency in monodisperse systems is usually nonlinear- scaling as $f^{1/2}$ at low frequencies and as f^4 at high frequencies.

There are two possible explanations for this phenomena. The system could be in an intermediate state between the viscous and scattering regions where attenuation scales roughly linearly with frequency. Although possible, this explanation is unlikely because any such behavior would likely be confined to a small range of frequencies. The

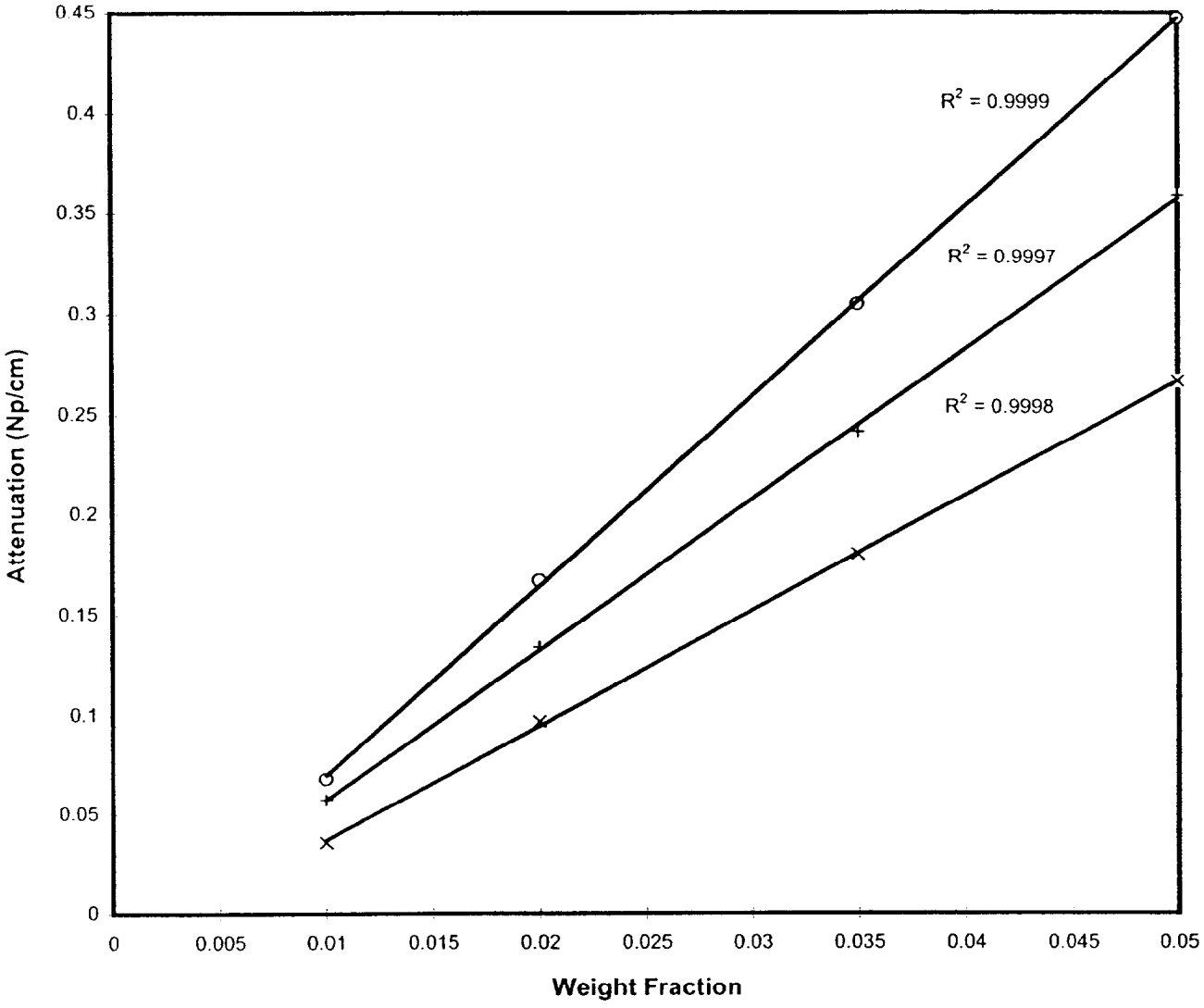

Figure 5.8: Attenuation versus volume fraction for slurries of clay (2 parts kaolin to one part Bentonite, by weight) in water at three frequencies. The frequencies studied are (o) 12 MHz, (+) 10 MHz, and (×) 8 MHz.

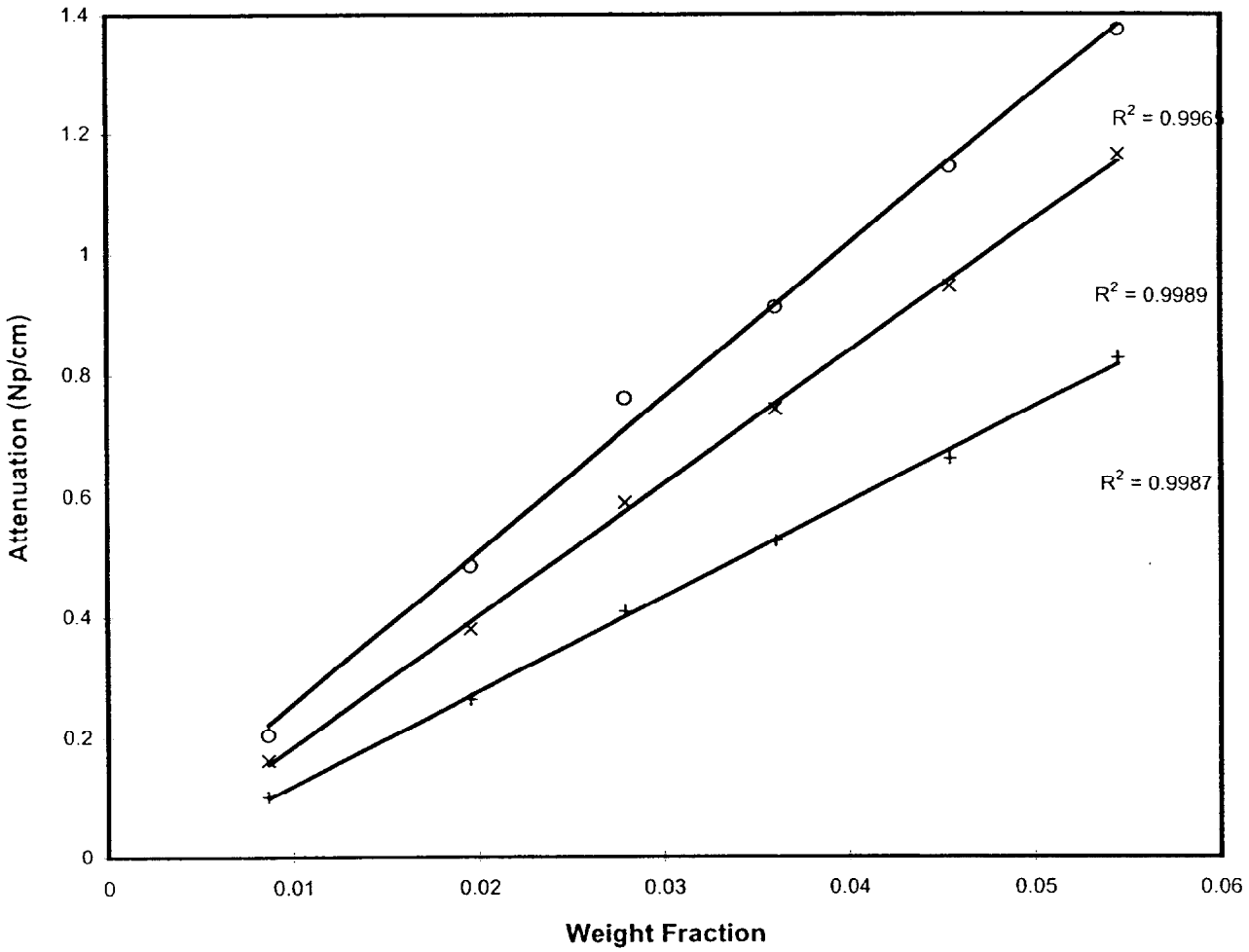

Figure 5.9: Attenuation versus volume fraction for crystallized salt solution system at three frequencies. The frequencies studied are (o) 12 MHz, (×) 10 MHz, and (+) 8 MHz.

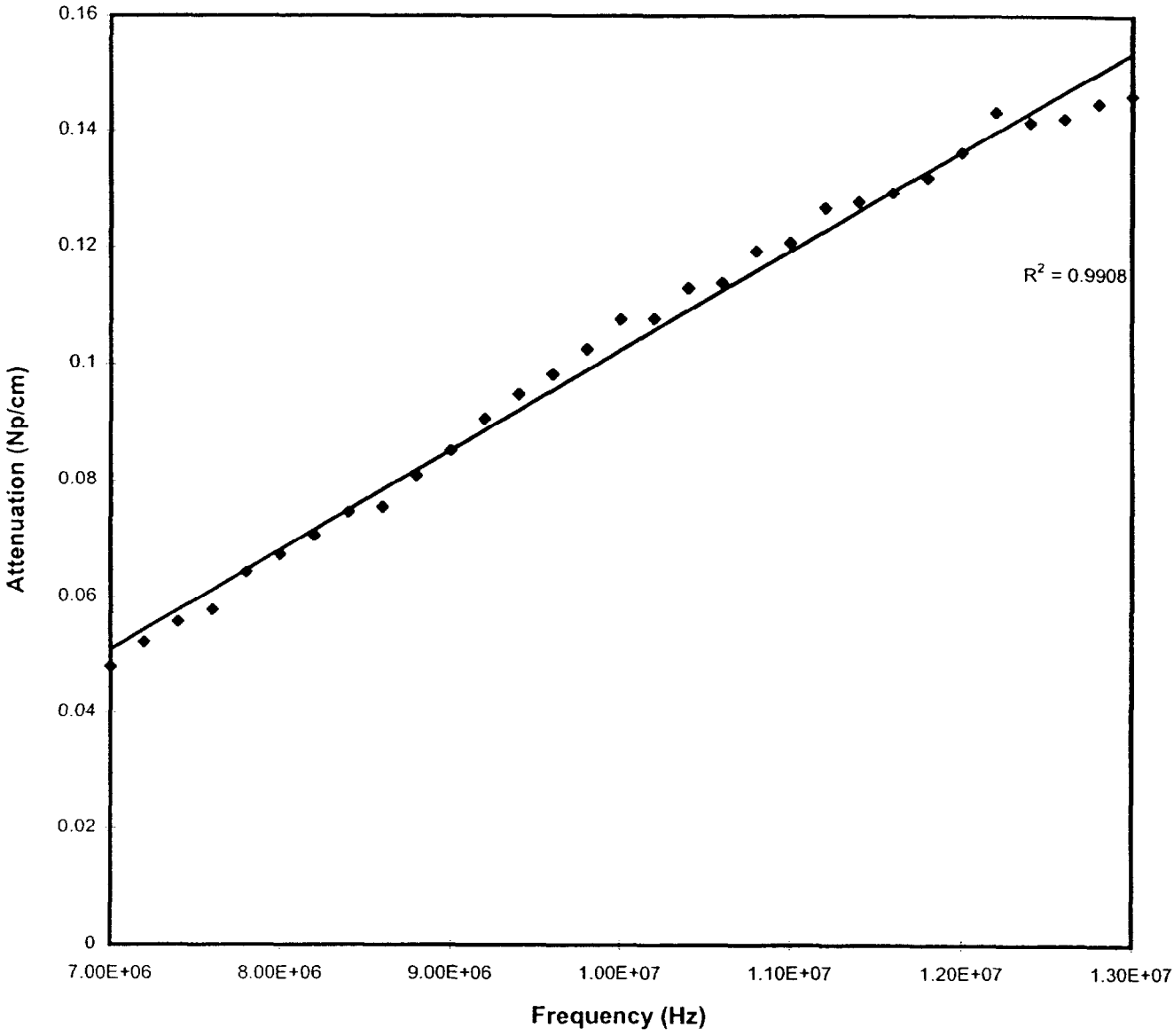

Figure 5.10: Attenuation versus frequency for crystallized salt solution. Points represent experimental data, the line is a linear fit.

attenuation behavior was linear across a relatively broad frequency band (7-13 MHz). It is unlikely that a system would be in a transition region over this range.

A more likely explanation is that the system is highly polydisperse. If the solids are composed of small particles with a few much larger particles then an approximately linear relationship could result. Small particles would have a small $k_{cl}a$ and be in the viscous or thermal attenuation range. Larger particles would have a $k_{cl}a$ closer to unity where scattering effects are more dominant. The combination of the two could produce a pseudo-linear relationship.

To explore the issue of a polydispersed system, an effort was made to estimate the particle size distribution using a microscopic particle size analysis. A sample of diluted slurry is dried on a slide and examined under a microscope. It is observed that there are two types of solids - small (~10 μm in length) needle-like particles and larger (~100 μm diameter) cubic crystals. Particle size distribution, shown in Table 5.1, is calculated from photographs of the system. See Figure 5.11 for photographs of the large particles and the small particles. The system is calibrated by taking photographs of a precision gradicule.

Particle Size Range (Diameter, μm)	Volume Fraction (n = 161 particles)
0-38	0
38-77	0.04
77-115	0.28
115-154	0.33
154-192	0.19
192-230	0.10
230-270	0.03
270+	0.04

Table 5.1: PSD of CSS solids

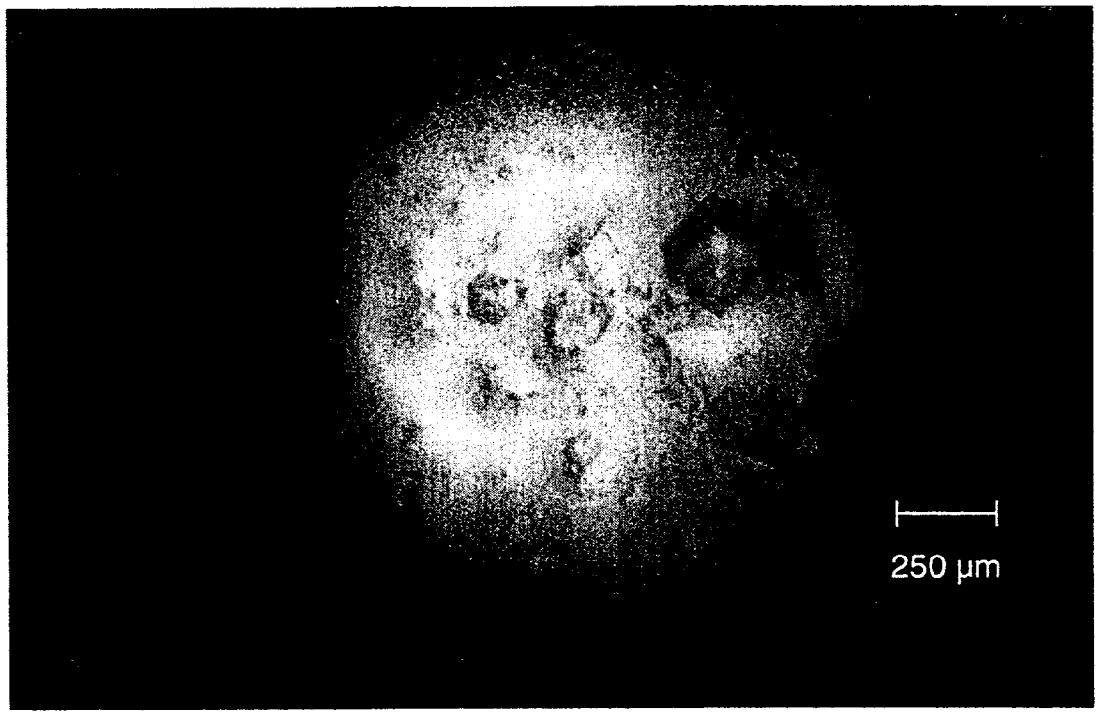

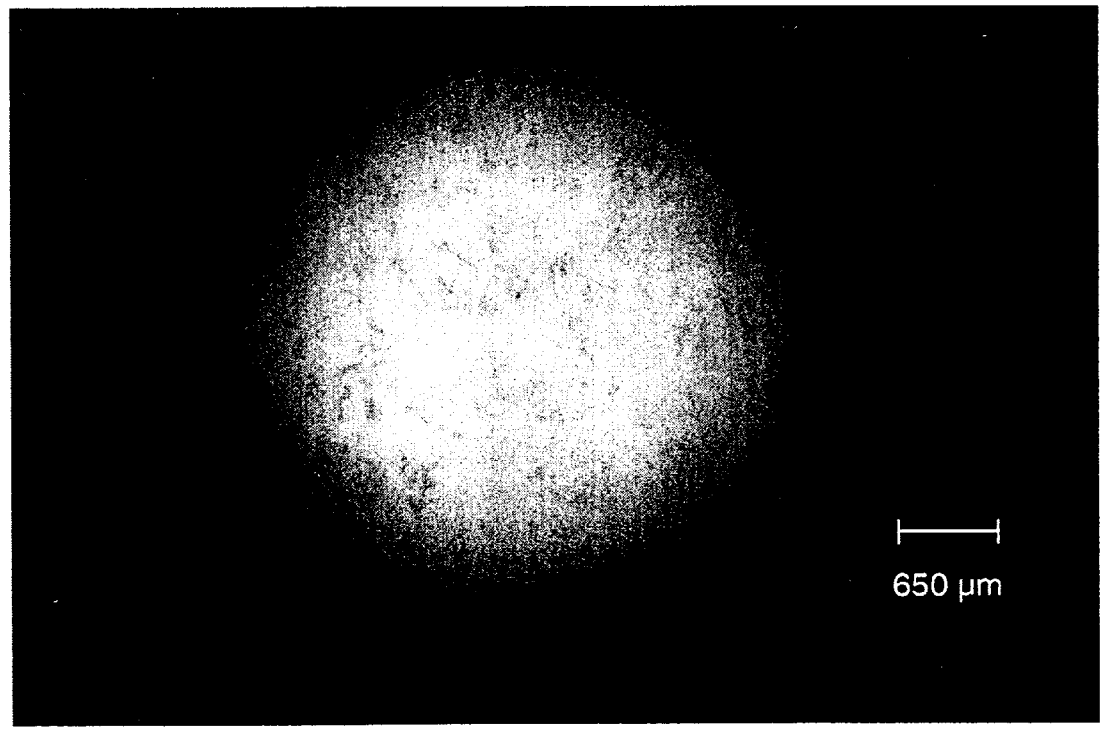

Figure 5.11: Photographs of crystallized salt solution particles. The photograph on top shows the larger particles, at a magnification factor of approximately 50. The photograph on the bottom shows the smaller particles, at a magnification factor of approximately 130.

No particle size distribution is available for the needlelike particles as they are too small to accurately measure (particularly their diameter) with the apparatus available. The approximate average length appear to be 10 μm.

5.3.1 COMPARISON WITH THEORY

The program used to estimate attenuation for the soda-lime glass system is for monodisperse particles, and cannot be used with the surrogate. Instead, a program that considers different particle sizes is used. Since the surrogate system is significantly different physically from the water / glass bead system a number of physical constants have to be changed. The values used are shown in Table 5.2:

	Solid	Supernate
Density (g/cm^3)	2.2 (a)	1.48 (b)
Thermal Conductivity ($J/K \cdot cm \cdot s$)	9.6×10^{-3} (c)	5.87×10^{-3} (c)
Specific Heat ($J/g \cdot K$)	0.836 (c)	4.19 (c)
Thermal Expansion Coefficient (K^{-1})	3.2×10^{-6} (c)	2.04×10^{-4} (c)
Attenuation Coefficient per f^2 (s^2/cm)	1.0×10^{-15} (c)	2.5×10^{-16} (c)
Sound Speed (cm/s)	5.2×10^{5} (c)	2.14×10^{5} (b)
Shear Viscosity ($g/cm \cdot s^2$)	-	1.48×10^{-1} (b)
Shear Rigidity ($g/cm \cdot s^2$)	2.8×10^{11} (c)	-

Table 5.2: Physical constants used for theoretical calculations for CSS system.
a: estimated (Weast, 1972)
b: measured
c: Taken to be the same as that for soda-lime glass beads

Note that due to the nature of the surrogate system several parameters could not be measured. They are instead estimated using average values of sodium salts given in Weast (1972) or taken to be the same as those of the soda-lime glass / water system.

Attenuation is a linear function of volume fraction at low volume fraction so only one volume fraction needs to be used for comparison. All computer simulations are run with a total solid volume fraction of one percent.

As a first approximation the system is taken to have two particle sizes - small (5 μm radius) and large (50 μm radius). The parameter varied is the ratio of the volume fractions of the two particles. As shown in Figure 5.12, a ratio of 70% (volume) smaller particles to 30% (volume) larger particles is consistent with experimental data.

Efforts to more accurately characterize the surrogate system using the measured particle size distribution met with mixed success. The two particle model explained above was modified so that the smaller particles were still taken to be spheres of 5 μm radius, while the larger particles were of several particle sizes as shown in Table 5.1. As shown in Figure 5.13, the predicted behavior is not as linear as that found using the model which assumed two particle sizes. This could be due to several factors. As mentioned previously, not all physical parameters of the slurry system can be measured. Some have to be estimated (see Table 5.2). In addition, it is not possible to get detailed information on the smaller particles size distribution. Finally, it is not possible to determine experimentally the ratio between the small and large particles.

5.4 REPRODUCIBILITY OF DATA

Several replicate runs were performed in order to gauge the reproducibility of the data for attenuation versus volume fraction plots. Four replicate experiments are performed on each of the three systems: SLG, BKC, and CSS. Fresh slurries were prepared for each experiment. No slurries were reused. Reproducibility of all three systems was acceptable, as shown in Figure 5.14. The SLG and CSS systems showed

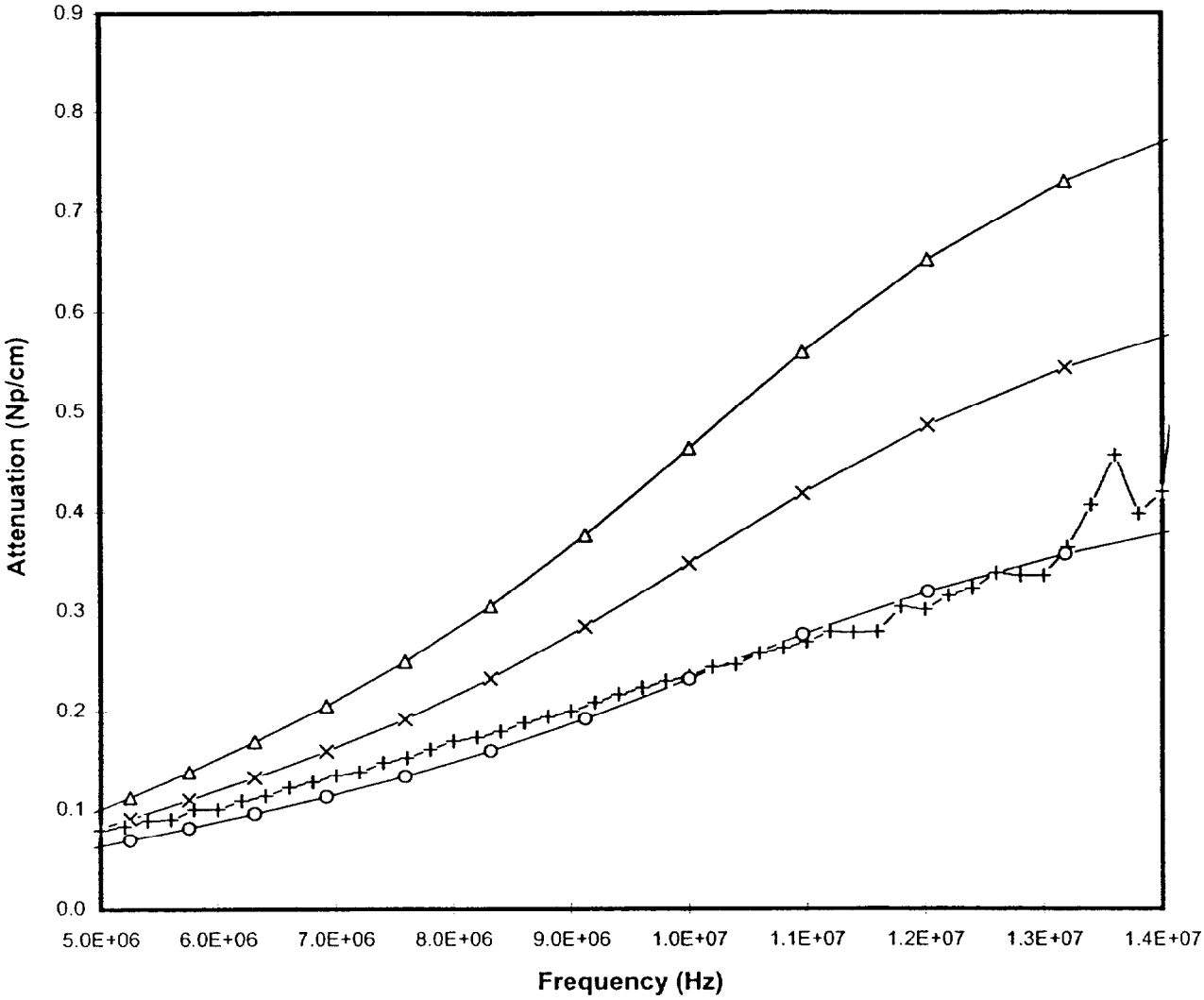

Figure 5.12: Results of the two particle size model to predict attenuation in the crystallized salt solution. It was assumed that the solids had two particle sizes, a smaller size with radius of 5 μm and a larger size with a radius of 50 μm. The ratio of the two particle sizes was varied. Volume fraction ratios shown (5 μm:50μm) are: (o) 30:70, (×) 50:50, and (Δ) 70:30. (+) represents experimental data.

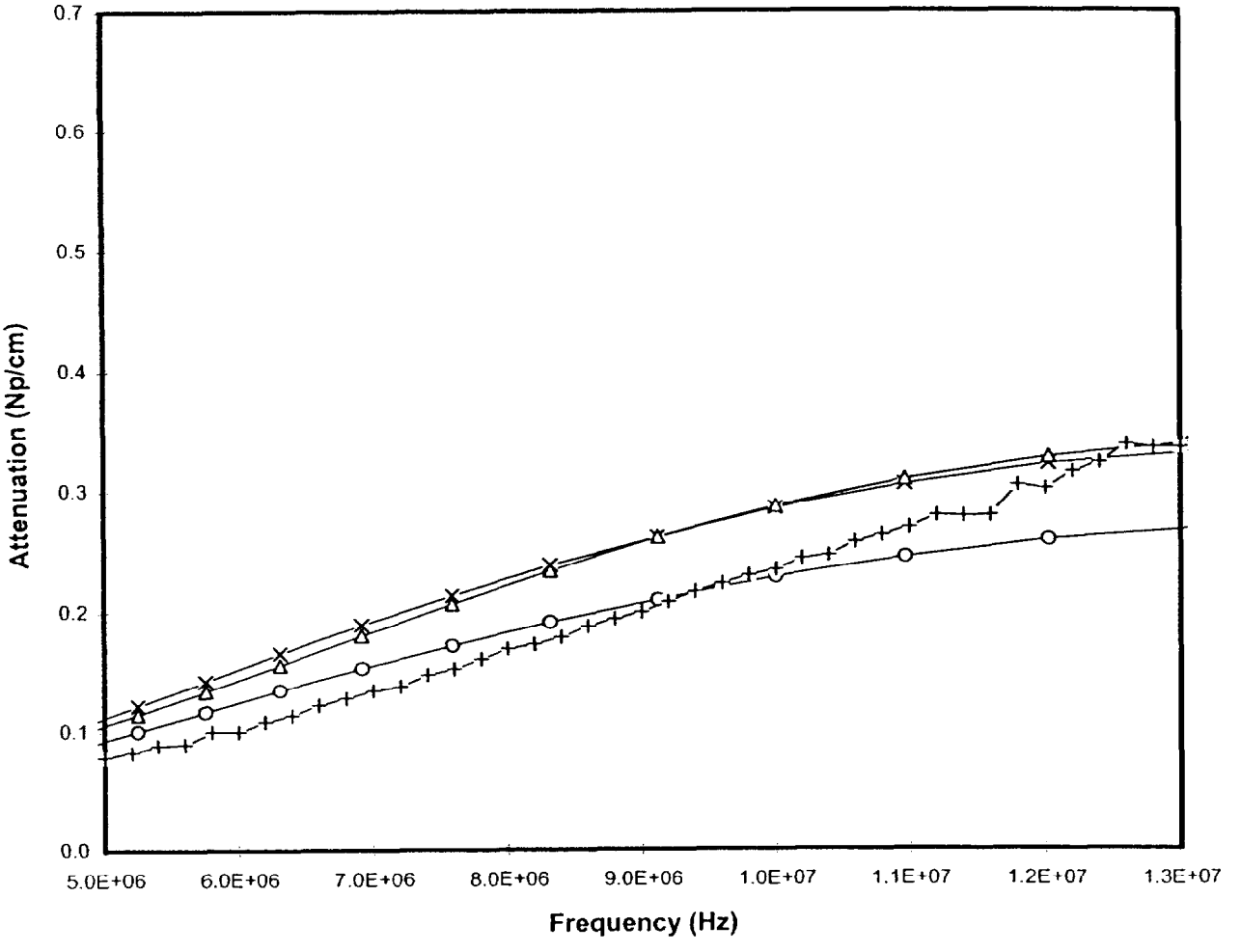

Figure 5.13: Results of expanding the two particle size model to predict attenuation in crystallized salt solution to include actual measured particle size information. Again it was assumed that the solids were of two different types. The first type was still taken to be spheres of radius 5 μm. The larger particles were of various sizes, as shown in Table 5.2. Volume fraction ratios shown (5 μm:larger particles) are: (+) 30:70, (Δ) 50:50, and (×) 60:40. (+) represents experimental data.

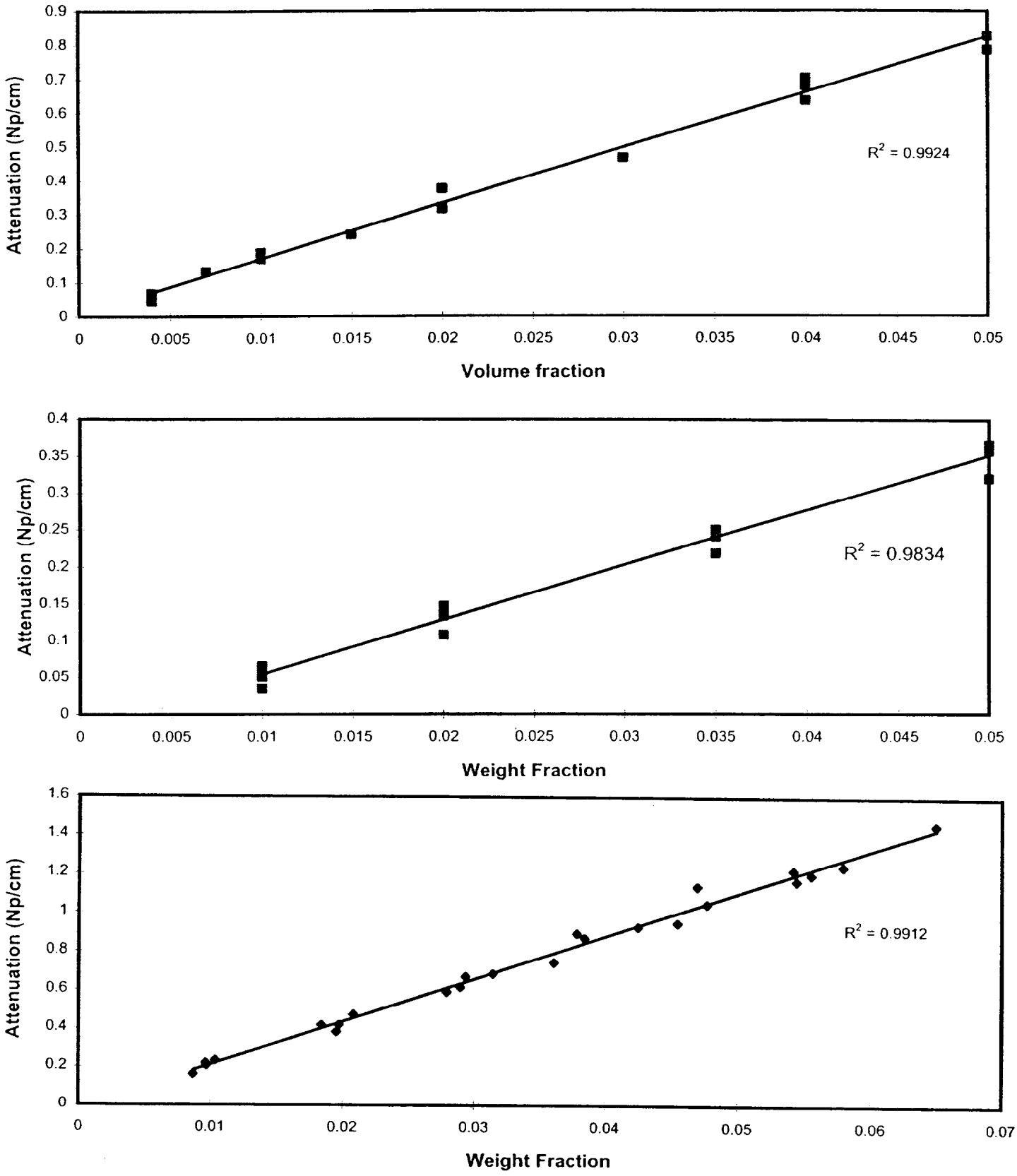

Figure 5.14: Reproducibility of data in liquid solid systems. Four experimental runs were performed on each system, with new slurry prepared for each run. All data is at 10 MHz. Systems shown are (top) SLG, (middle) BKC, (bottom) CSS.

similar amounts of scatter, having R^2 values of 0.992. The BKC system displayed slightly more scatter, with an R^2 value of 0.983.

5.5 SPEED EXPERIMENTS

Figure 5.15 shows the effect of volume fraction on ultrasonic speed in the soda-lime glass system and the Potter's bead system at a frequency of 2.25 MHz over a broader range of volume fractions (0.0 to 0.4). The behavior is nonlinear as expected. The speeds measured in the two systems are roughly similar. The greatest deviation is present when volume fractions are low, less than 20%. The speed in the Potter's beads is less than the speed in the soda-lime glass beads. This is likely due to experimental error. Large particles settle much faster than small particles, particularly at low volume fractions, and it is very difficult to keep the slurry homogenous. The effective volume fraction seen by the transducers could be lower than the actual volume fraction, causing the measured speed to be lower than expected.

Figure 5.16 shows the results of the low volume fraction speed experiments. The linear fit is acceptable but practical considerations decided against further consideration of using phase speed to characterize low VF slurries. At low volume fractions the change in speed due to the solids is very small (less than 10 m/s, or 0.7% of the total speed) and any change in temperature or any non-uniformity of the slurry is significant.

No speed experiments were performed with the CSS system. In order to calculate the theoretical attenuation in the CSS system the ultrasonic speed in the supernate is measured. The value is found to be quite high - ~2200 m/s, and rather close to the expected speed in the salt (~2500 m/s). Thus any change in speed due to the presence of

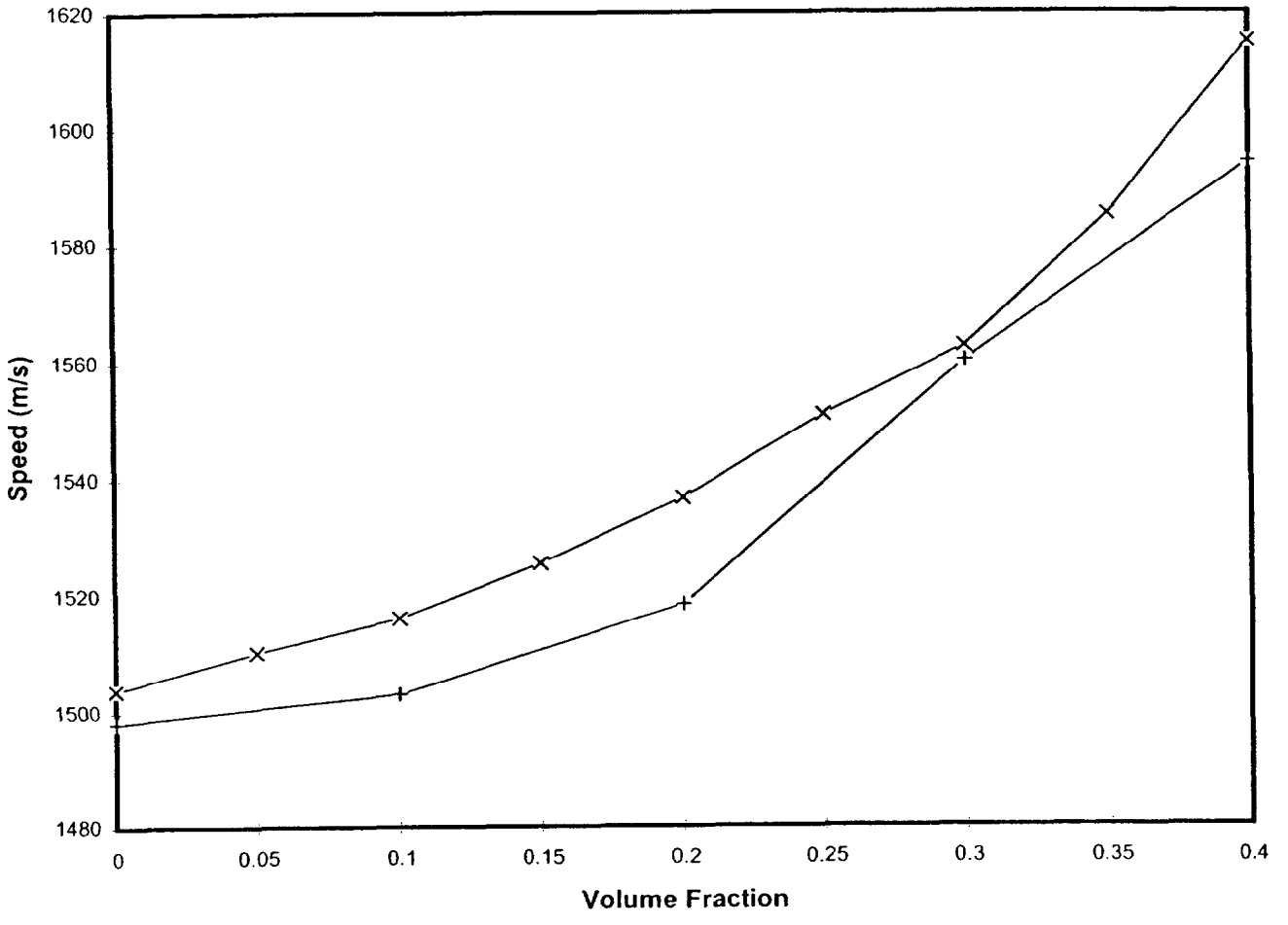

Figure 5.15: Effect of volume fraction on phase speed in solid-liquid slurries. Particles are (×) Soda lime glass (r = 16 μm) and (+) Potter's beads (r = 60 μm). Volume fraction ranges from 0.0 to 0.4.

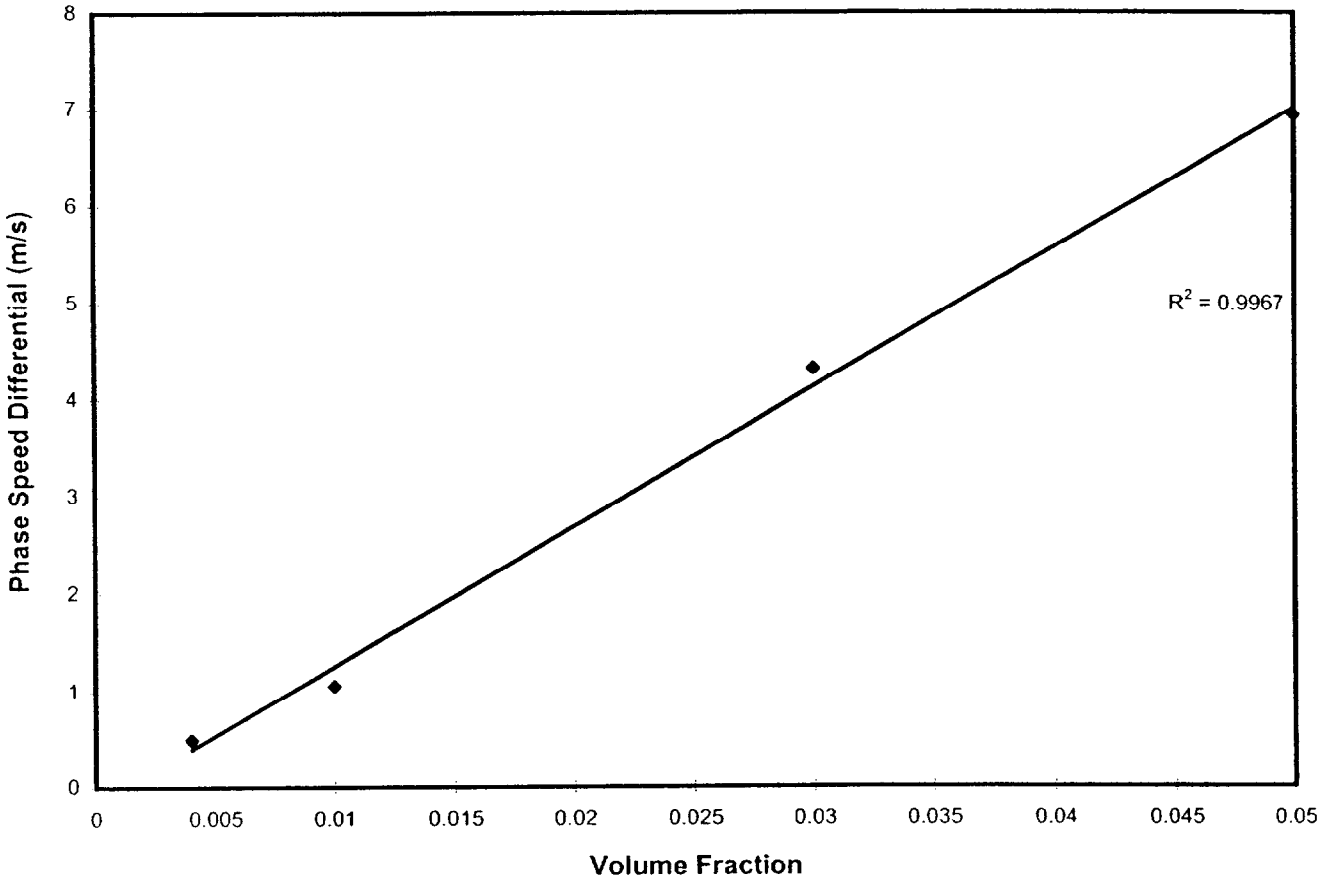

Figure 5.16: Phase speed differential versus volume fraction for low volume fraction soda-lime glass beads. The phase speed differential is the difference between the phase speed in slurry and the speed in the suspending liquid (water). Data is represented by points. The line is a linear fit.

salt would be very small and difficult to measure, particularly at low volume fractions. Accordingly, these measurements were not made.

5.5.1 COMPARISON WITH THEORY

Figure 5.17 compares the speed measured in soda-lime glass beads with the speed predicted by the computer simulations. The simulation agrees very well with the experiment. These results demonstrate that the basic premises of the theory hold for this system over a wide range of volume fractions.

6. Conclusions

The following conclusions can be drawn from this study.

The acoustic monitor is shown capable to accurately measure volume fraction of solid-liquid slurries in low concentration ranges of 0.4 to 10 volume percent by analysis of the attenuation of the transmitted wave. A linear relationship exists in this region between attenuation and volume fraction for three slurry systems studied: a) soda-lime glass beads in water (SLG), (b) a physical radioactive waste slurry surrogate of Bentonite and kaolin clay in water (BKC), and (c) a chemical radioactive slurry surrogate consisting of a crystallized salt solution in supernate (CSS). This relationship exists in the presence of small amounts of gas bubbles when the frequencies of interrogation are much greater than the resonance frequency of the gas bubbles. The frequency ranges studied are 8 MHz to 12 MHz for all three systems. Replicate experiments conducted for the three systems demonstrate linear behavior with regression coefficients of 0.983 to 0.992.

The theory developed by Spelt et al. (2000) describes well the attenuation-frequency behavior for the well characterized SLG system for 0.4 to 5 volume percent

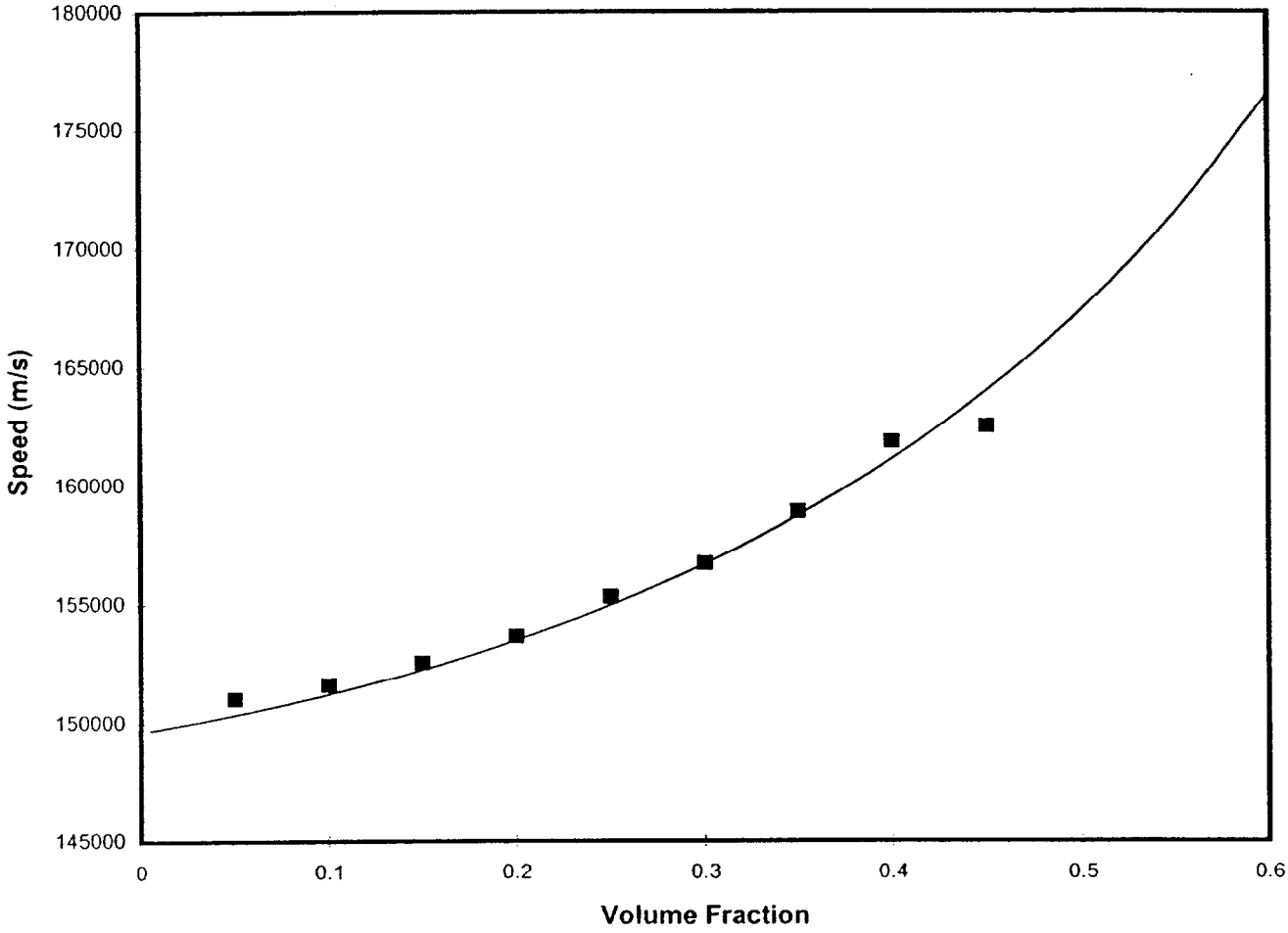

Figure 5.17: Comparison of measured phase speed with theoretical phase speed. Experimental data is represented by points, while the line represents theoretical calculations. Frequency is 2 MHz, temperature 25 °C.

slurries. Attempts to apply the theory to the CSS system met with limited success due to the complexity of the salt crystals morphologies (at least two different crystal structures exist, each with broad particle size distributions), and unknown physical properties of these crystals are estimated.

The sender-receiver mode experimental setup using pairs of transducers mounted in a slurry sample cell is employed with fast Fourier transform analysis to obtain the attenuation measurements. The technique is the same as that employed earlier by Norato (1999) and provides accurate results.

Acoustic speed through the well characterized SLG slurries can be accurately measured using the reflectance method adapted from McClements (1991) for a broad range of volume fractions of 5.0 to 40 percent. With proper control of temperature, speed can be measured to ±0.3 m/s. The theory of Spelt et al. (2000) is in close agreement with these data. For low volume fractions (less than 10 volume percent) accurate data can be produced with very careful monitoring of temperature. These results show that the reflectance method and theory can be a valuable tool to characterizing solids content if solid-liquid slurries at large volume fractions.

7. Future Work

Future work involves automating the procedure to measure attenuation and manufacturing an on-line monitor on spoolpiece to characterize flowing slurries. The basic experimental setup will be similar to that currently employed, except the procedure will be automatic, controlled by a computer. A computer controlled pulser/receiver will be used to generate the spike pulse. The pulse will then be routed through a high voltage,

high bandwidth computer controlled multiplexer to the appropriate transducers. The multiplexer will act as a switchbox, enabling the use of several different transducers without having to manually change the signal wires. The signal will be read on a digital oscilloscope card installed in a PC and attenuation will be calculated automatically.

The baseline signal will be acquired continuously, using the same system used to acquire the sample signal. A Mott® filter will be used to separate the solids from the liquid stream. This stream will pass through a transducer bank and be interrogated by the appropriate transducer pairs before being returned to the slurry line. See Figure 7.1 for a schematic of the wiring setup and the spoolpiece.

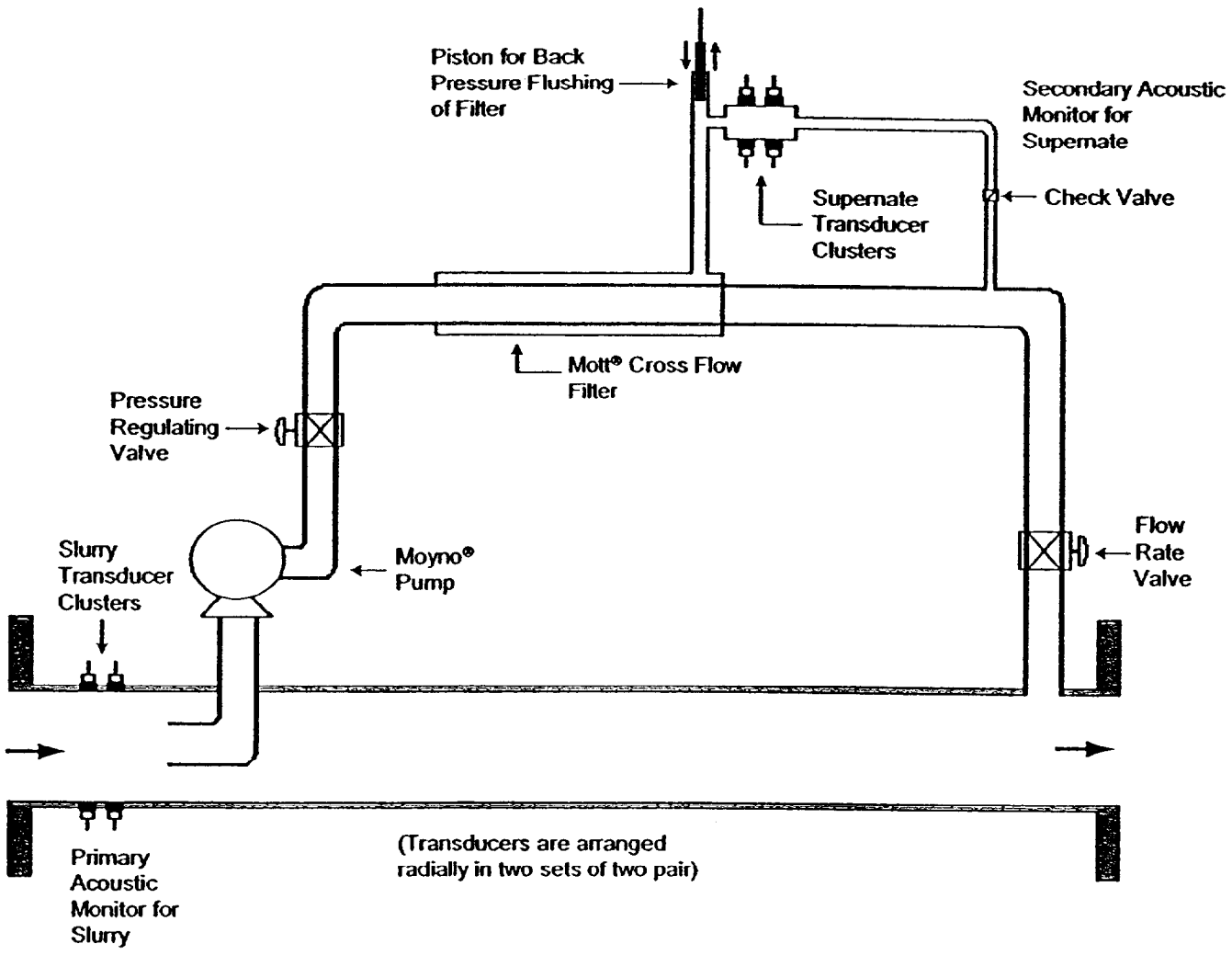

Figure 7.1: Conceptual Diagram of Acoustic Monitor on Spool Piece. The unit includes the primary acoustic monitor transducer cluster for slurry; and the by-pass loop with slurry pump, cross-flow slurry filter with pressure actuated backflush piston, and secondary acoustic monitor with interrogative cell for supernate.

References

Allegra, J.R. and Hawley, S.A., "Attenuation of sound in suspensions and Emulsions: Theory and experiments," *J. Acoust. Soc. Am.* **51**, 1545 (1972).

Atkinson, C.M. and Kytomaa, H.K., "Acoustic wave speed and attenuation in suspensions," *Int. J. Multiphase Flow.* **18**, 577 (1993).

Bolz, R.E., *CRC Handbook of tables for Applied Engineering Science* (CRC Press, Boca Raton, FL, USA, 1973).

Cowan, M.L., Beaty, K., Page, J.H., Liu, Z., and Sheng, P, "Group Velocity of Acoustic Waves in Strongly Scattering Media: Dependence on the Volume Fraction of Scatterers," *Physical Review E.* **58**, 6626 (1998)

Epstien, P.S. and Carhart, R.R., "The absorption of sound in Suspensions and Emulsions. I. Water Fog in Air," *J. Acoust. Soc. Am.* **25**, 553 (1953)

Golcar, G.R., Colton, N.G., Darab, J.G., and Smith, H.D., "Hanford Tank Waste Simulants Specifications and Their Applicability for the Retrieval, Pretreatment, and Vitrification Processes," PNWD-2455/BNFL-RPT-012 Rev. 0, 2000.

Grim, R.E., *Clay Minerology* (McGraw-Hill Book Company, New York NY, USA, 1968, pg. 567.

Greenwood, M.S., Mai, J.L., and Good, M.S., "Attenuation Measurements of Ultrasound in a Kaolin-Water Slurry: A Linear Dependence Upon Frequency," *J. Acoust. Soc. Am.* **94**, 908 (1993).

Holtz, R.D., and Kovacs, W.D., *An Introduction to Geotechnical Engineering* (Prentice-Hall, Inc., Englewood Cliffs, NJ, USA, 1981, pp. 81-82

Hudson, J.D., "Defining Waste Acceptance Criteria for the Hanford Replacement Cross-Site Transfer System," PNNL-11146/UC-2030, National Technical Information Service, 1996

Hylton, T.D., and Bayne, C.K., "Testing of In-Line Slurry Monitors and Pulsair Mixers with Radioactive Slurries," ORNL/TM-1999/111, National Technical Information Service, 1999

Hylton, T.D., "An Evaluation of a Dual Coriolis Meter System for In-line Monitoring of Suspended Solids Concentrations in Radioactive Slurries," ORNL/TM-2000/184, National Technical Information Service, 2000.

Kinsler, L.E., Frey, A.R., Coppens, A.B., and Sanders, J.V., Fundamentals of Acoustics (John Wiley & Sons, Inc., New York, NY, USA, 1982).

McClements, D.J., "Characterisation of Emulsions Using a Frequency Scanning Ultrasonic Pulse Echo Reflectometer," *Proc. Inst. Acoust.*, **13**, 71 (1991).

Norato, M.A., "Acoustic Probe for the Characterization of Solid-Gas-Liquid Slurries," Ph.D. Thesis, Syracuse University (1999).

Spelt, P.D.M., Norato, M.A., Sangani, A.S., Greenwood, M.S., and Tavlarides, L.L., "Attenuation of Sound in Concentrated Suspensions: Theory and Experiments", *J. Fluid Mechanics.*, **420**, 1 (2000)

Spelt, P.D.M, Imperial College, London, England. Private Correspondence. July-September 2000.

Tsouris, C., Norato, M.A., and Tavlarides, L.L., "A Pulse-Echo Ultrasonic Probe for Local Volume Fraction Measurements in Liquid-Liquid Dispersions," *I & EC Res.* **34**, 3154 (1995).

Weast, R.C., CRC Handbook of Chemistry and Physics (The Chemical Rubber Co., Cleveland, OH, USA, 1972).

Appendix A:
Procedure for synthesizing Crystallized Salt Solution

The procedure used to synthesis the surrogate slurry follows. Source is Golcar (2000), although a few changes were necessary due to equipment limitations.

Simulant ID: SY1-SIM-91A

The simulant is prepared by evaporating (under reduced pressure) excess water from a dilute feedstock solution.

Feed Solution Preparation:

1. Weigh out the following:

Compound	g needed for 1-L of feedstock
NaOH	64.4
NaAl(OH)4	126.23
NaNO2	154.56
NaNO3	220.12
Na2CO3	45.15

2. To make 1L of solution use a 2 L beaker, starting with about 500 ml water. Use a round Teflon stir bar for agitation.
3. Heat water to about 90 C and add sodium aluminate. Stir and heat until the solution is almost clear; waiting too long results in the precipitation of aluminum hydroxide.
4. Turn off heat and slowly add NaOH pellets.
5. Add sodium carbonate and stir until dissolved. Some cooling may be necessary to get all the carbonate into solution.
6. Turn heat back on and add sodium nitrite followed by sodium nitrate
7. Add water when necessary to dissolve solids, trying to have a total of 900 ml solution when finished.

Slurry Preparation:

The solution prepared above is evaporated down in a RotoVap until the final volume is ~700 ml.

1. Assemble RotoVap instrument with accessory hot water bath. Connect vacuum line to house vacuum. Connect condenser water line to house cold water.

2. Fill RotoVap vessel with 700 ml water, mount in RotoVap, and mark water line on outside of vessel with a permanent marker. The purpose of this line is to gauge when to stop the RotoVap process. When the slurry level comes even with the marked line then the process is over, as the desired volume of 700 ml is reached.

3. Fill water bath so that water level is 1 cm from the inside lip, with the RotoVap vessel immersed. Set water bath to 90°C.

4. Begin evaporation. Set rotation level at the 9:30 position (~65 rpm).

5. Stop evaporation once slurry level reaches the mark placed in step 2.

6. Allow to cool with stirring overnight.

Slurry Separation:

The slurry is separated in a centrifuge (Fisher Marathon 21000 CF). Slurry is placed in centrifuge beakers and spun until all solids have settled. The supernate is then carefully drawn of. The solids are collected and centrifuged again.

1. Fill four 200 ml centrifuge beakers with slurry. Using balance verify that the mass of all four vessels is within one gram of each other.

2. Centrifuge 20 minutes at 2000 RPM.

3. Carefully pipette solid-free supernate into storage vessel. Leave approximately 1 cm of supernate on top of settled solids.

4. Combine all solids and centrifuge again (2000 RMP, 10 minutes), using a beaker filled with water as a counterweight.

5. Carefully pipette solid-free supernate into storage vessel. Stop placing the supernate into the vessel when it appears that solids are being drawn into the pipette with the supernate.

6. Remove all remaining supernate and discard. Transfer wet solids into storage container.

Appendix B:
Transducer Specifications

All transducers are produced by Panametrics, Inc. (Waltham, Ma) and are Videoscan immersion transducers.

Model Number	Serial Number	Element Diameter (cm)	Center Frequency (MHz)	Bandwidth (- 6 dB) (%)	Operating Range (MHz)
V302	211353	2.54	0.935	65.24	0.6 to 1.4
V302	211354	2.54	0.950	65.26	0.6 to 1.4
V304	217679	2.54	2.11	63.51	1.4 to 3.0
V304	217680	2.54	2.08	63.46	1.4 to 3.0
V308	219594	1.90	4.88	56.41	3.0 to 7.0
V308	237702	1.90	4.65	60.22	3.0 to 7.0
V320	222752	1.27	7.95	64.15	5.0 to 11.0
V320	222753	1.27	8.05	55.90	5.0 to 11.0
V311	221617	1.27	9.90	64.65	6.0 to 12.0
V311	266829	1.27	10.4	48.80	6.0 to 12.0

Appendix C:
Speed Measurement Procedure

B.1 Slurry Speed Measurement Procedure:

For a detailed explanation of the pulse echo technique see McClements and co-workers (1990, 1991). The following procedure describes all steps necessary to measure sound speed in liquids.

Data Acquisition:

1. Turn on cooling water and water bath. Set water bath temperature to 26°C. The test cell is constructed of thick Plexiglas® which resists heat conduction so it is necessary to have the water bath at a slightly higher temperature than that desired for the slurry.

2. Assemble test cell. Choose pathlength desired (½" or 1") and install appropriate reflector plate to back of test cell. Choose transducer required and place in appropriate mount, taking care that the transducer surface is flush with the mount. Tighten set screw when using 7.5 or 10 MHz transducer. Apply a small amount of ultrasound gel to transducer well in test cell. Clamp mounted transducer to test cell using supplied screws, taking care to tighten each side gradually.

3. Attach co-axial wire to transducer and 5052 PR Pulser Receiver.

4. Fill cell with slurry, place in water bath and allow to come to desired temperature (25°C). Monitor sample temperature with digital thermometer.

5. Turn on oscilloscope. Refer to Norato (1999) for instructions on operating oscilloscope.

6. Verify that 5052PR is set to pulse-echo mode. Switch labeled "1/2" should be set to "1".

7. Check fixed settings of 5052PR. Rep rate should be set to zero (minimum setting but not on "EXT"). Gain should be set to 40 dB. H.P. filter should be set to "out".

8. Set variable settings of 5052PR. Energy, attenuation, and damping are varied depending on transducer used and experimental conditions: Refer to Table C.1 below for a starting setting for each transducer:

Transducer	Energy*	Attenuation	Damping
1 MHz	4	46	0
2.25 MHz	4	46	4
5 MHz	3	48	10
7.5 MHz	1	36	10
10 MHz	1	4	10

Table C.1: Suggested settings of Pulser/Reciever.
* Energy should not be set above 3 for transducers of centerline frequency 5 MHz or greater.

9. Fine tune variable settings of 5052PR. The goal is to create a spike pulse with as high an amplitude as possible, that is not squared off when viewed on the oscilloscope. Additionally, damping should be set such that the baseline voltage is near zero before the first echo is received by the oscilloscope. Once damping is set properly vary attenuation until either the first or second echo waveform begins to square off. Then increase attenuation by four.

10. Check math settings of oscilloscope. Correct settings are:
    Trace (A) - Summed average of Channel 1, 50 sweeps
    Trace (B) - Functions, Negation of M1
    Trace (C) - Phase FFT of (A)
    Trace (D) - Phase FFT of (B)

11. Gather waveforms. Center second echo in oscilloscope. Have Volts/Division set such that the entire waveform takes up about 1/3 of the window, but take care that any echoing waveforms are not displayed. Activate Trace A and Clear Sweeps to take new reading. Then go to Waveform Store and store A to M1.

12. Center first echo in oscilloscope, with all settings equal to those used in the previous step. Activate Trace A and Clear Sweeps to take reading.

13. Perform FFT Operation. Turn off Channel 1 and turn on Trace (A) and (B). Superimpose waveforms on the main peak of both waveforms. It is helpful to zoom in when doing this. Using cursors, determine the time of the main peak of both waveforms and record. Keeping the waveforms superimposed, zoom out and activate Trace (C) and Trace (D).

14. Save FFT data. Turn off Trace (A) and Trace (B). Insert floppy disk in drive. Go to Waveform Store and set "to FLPY" (floppy). Set Data Format to ASCII, MathCad Format. Store "All Displayed" to "FLPY" and press "Do Store". For more information on storing waveforms to floppy see Norato (1999).

Calculations:

Calculations are performed in MS Excel. There is a template file for performing phase speed calculations named PSPEED.XLS, located in the C:\PSPEED directory.

1. Open PSPEED.XLS in MS Excel. Immediately save file as different filename. Do not make changes to PSPEED.XLS before saving it as a different filename.

2. Follow instructions in spreadsheet. Fill in experimental conditions and peak times recorded earlier. Open FFT data files and cut and paste data.

3. In order to correctly subtract the phase information given by the FFT procedure all phase angles must be positive. Therefore make corrections of +360° to all negative phase angles.

4. Phase speed is now automatically calculated and displayed in column labeled "Phase Speed".

Acoustic Probe for the Characterization of Solid-Gas-Liquid Slurries

by

Michael Anthony Norato
B.S. Ch.E., Syracuse University, 1991
M.S. Ch.E., Syracuse University, 1994

DISSERTATION

Submitted in partial fulfillment of the requirements for the degree of Doctor of Philosophy in Chemical Engineering in the Graduate School of Syracuse University

May 1999

Approved Lawrence Tavlarides
Professor Lawrence L. Tavlarides

Date Feb/17/99

Acoustic Probe for the Characterization of Solid-Gas-Liquid Slurries

by

Michael Anthony Norato

Abstract of Dissertation

May 1999

The development of nuclear weapons technology during the Cold War Era has left a legacy of large quantities of radioactive waste which are stored throughout the US Department of Energy (US DOE) Nuclear Weapons Complex. During the proposed remediation stages of processing, it will be necessary to characterize and monitor these waste slurries by remote methods.

Acoustic probes have shown promise because of their non-intrusive nature and ability to penetrate optically opaque slurries.

A forward theory for the acoustic response in both dilute and concentrated solid-liquid slurries is developed. It is based on ensemble averaging of the equations of motion in the solid and liquid phases to obtain expressions for the "effective properties" of the slurry mixture in terms of coefficients which appear in the equations of motion for the solid particle. The attenuations predicted from the theory are in generally good agreement with the experimental data obtained by Toneburst and Pulse/FFT data acquisition methods for solid-liquid slurries of soda-lime glass particles of 14.9 μm and

65 μm mean radius and polystyrene particles of 79 μm radius at concentrations ranging from 5 % to 50 % solids by volume.

The forward theory is readily extended to systems containing more than one dispersed phase, such as particles and gas bubbles, and the theory predictions are observed to be in good agreement with preliminary attenuation data obtained in solid-gas-liquid slurries of soda-lime glass particles of 14.9 μm mean radius at 5 % and 10 % by volume and gas bubbles ranging from approximately 25μm to 150 μm radius at volume fractions on the order of 10^{-5}.

An inverse theory is also developed to determine the concentration and solids volume fraction distribution in a solid-liquid slurry given its experimentally obtained acoustic response. A Tikhonov scheme is employed to regularize the ill-posed integro-differential equations and solve them as a linear programming problem. Solution of the inverse problem is found to be successful in several cases, but the results are observed to be sensitive to the choice of frequency range, the physical properties of the particles, and the nature of the particle volume fraction distribution.

Table of Contents

List of Tables

List of Figures

Acknowledgments

I would like recognize and thank the following individuals for their indispensable contributions to the completion of this work:

Professor Lawrence L. Tavlarides, my research advisor, for his suggestions, criticism, and guidance, both personal and professional, throughout the course of this work, and indeed, my entire undergraduate and graduate education experience. I am very grateful for all he has done for me over the years.

Professor Ashok S. Sangani, my co-advisor on my doctoral research, for his assistance, guidance, and patience in the theoretical aspects of this work.

Drs. Margaret Greenwood and Stephen Doctor, and all the staff of the Non-Destructive Evaluation Section at the Battelle Pacific Northwest National Laboratory in Richland, WA, for the instruction, guidance, and friendship they provided during my four months at PNNL and throughout the course of this work.

Dr. Costas Tsouris, and all the staff of the Chemical Technology Division of the Oak Ridge National Laboratory, for the friendship, support, and assistance provided periodically throughout the course of this work. I would also like to thank his wife and colleague, **Professor Sotira Yiacoumi**, and her students at Georgia Institute of Technology for making some the early bubble size measurements used in this work.

Dr. Peter D.M. Spelt, for contributing his considerable talent in performing the theoretical portions of this work. I would also like to thank him for his advice, criticism, and friendship.

My parents, **Dr. and Mrs. Joseph F. Norato**, for their support and criticism throughout the years of my education.

Ella-Marie A. LaPlante, for her patience, understanding, love, and support. I know I did not always make it easy for her, but she stayed on through the final and most difficult year of my work...and for that, I am eternally grateful.

The technical and administrative assistance of the following people on various occasions is appreciated:

Technicians: Mr. John Banas, Mr. John Chabot, Mr. Dick Chave, Mr. Ronnie Judd, and Mr. John Kotlarz.

Students: Mr. Daniel Wright, Mr. Richard Henry, and Mr. Ted Hromadka (PNNL).

Administrative Staff: Mrs. Ruth Dewey, Mrs. Mickey Hunter, Mrs. Linda Lowe, and Ms. Linda Vanderhoof.

The financial support provided by the following organizations is greatly appreciated: Department of Chemical Engineering and Materials Science, Syracuse University.

The Graduate School of Syracuse University.

Associated Western Universities.

US Department of Energy, Environmental Management Science Program

Grant # DE-FG07-96ER14729.

Chapter 1: Introduction

1.1 Background

For nearly five decades, the US government has been building and stockpiling nuclear weapons without a well defined plan for the safe and permanent disposal of the highly toxic byproducts routinely created by the continual refining and manufacturing of plutonium and uranium (Garr 1992). The development and application of nuclear weapons technology during the Cold War Era has left a legacy of large quantities of radioactive waste which are stored throughout the fifteen facilities which comprise the US Department of Energy (US DOE) Nuclear Weapons Complex. The production of weapons grade nuclear materials began in the early 1940's and continued until the late 1980's. Nuclear weapons production efforts have generated 100,000 kilograms of plutonium. The PUREX (Plutonium Uranium Extraction) process creates more than 340 gallons of high-level radioactive waste and more than 55,000 gallons of low- to intermediate-level radioactive waste for every kilogram of plutonium produced (Garr 1992). Much of these wastes was stored with little or no documentation (Levi 1992), making characterization of the wastes an integral part of any potential remediation scheme.

It is estimated by the DOE that cleanup of the entire nuclear weapons complex will take thirty years and require about $100 billion, while some outside estimates predict that it will cost at least twice that much (Garr 1992). There are hundreds of waste storage

tanks across the US DOE Nuclear Weapons Complex that will require remediation in the next several decades. During the proposed retrieval, pretreatment, immobilization, and closure stages of the waste processing it will be necessary to characterize and monitor various properties of the resulting waste slurries by remote, non-intrusive methods. Real time monitoring of the size and volume fraction of solid particles in these slurries by acoustic probes has shown promise because of their (i) non-intrusive nature; (ii) simplicity of operation (unlike NMR and X-Ray tomography); and (iii) ability to penetrate concentrated and optically opaque slurries (unlike laser Doppler anemometry which requires refractive index matching).

Although acoustic probes have been commonly used for monitoring flows of single-phase fluids (McLeod 1967), their application to monitor multiple phase mixtures has not yet fully reached its potential. A number of investigators in recent years have been involved in developing probes for measuring the volume fractions in solid-liquid suspensions (Atkinson and Kytomaa 1993; Greenwood *et al.* 1993; Martin *et al.* 1995) and liquid-liquid dispersions (Bonnet and Tavlarides 1987; Tavlarides and Bonnet 1988; Yi and Tavlarides 1990; Tsouris and Tavlarides 1993; Tsouris *et al.* 1995). In particular, Atkinson and Kytomaa (1993) suggest that the acoustic technique can be used to determine both the velocity and the volume fraction of solids while Martin *et al.* (1995) claim that the acoustic probe can be used to obtain information on the size distribution of the particles. The acoustic probe is also used and commercially available (Malvern Instruments, Pen Kem, Inc.) for at-line (i.e., using samples or slip-streams drawn from a process line as opposed to on-line, implying simply being immersed in a mixing tank or

installed on a process pipeline) particle size measurements in solid-liquid slurries. Finally, an acoustic technique is also used for determining bubble size distributions in bubbly liquids (Duraiswami *et al.* 1998).

The work of the investigators just cited has established the potential of the acoustic probe for characterizing/monitoring two-phase flows in relatively ideal, well-characterized suspensions. One major obstacle to its wide-spread use in slurry processing, however, arises from the interference caused by the presence of small amounts of gas. The presence of a low volume fraction of gas bubbles formed, for example, by radiolytic degradation processes, cavitation from slurry pumps, or vapor entrainment could significantly interfere with the transmitted acoustic signal preventing straightforward application of a probe. Since the compressibility of the gas is typically several orders of magnitude greater than the compressibility of liquids and solids, the acoustic wave propagation is significantly affected even when the gas is present in relatively small amounts.

It may be possible, however, to overcome the interference introduced by the gas phase by carefully selecting the frequency range for interrogation and by making use of the theory of acoustic wave propagation in bubbly liquids in analyzing the acoustic response of the suspension. Since the gas bubbles are formed by a variety of different mechanisms and their size distribution in actual flows can vary considerably, an important problem to be solved is to determine the noise introduced by the bubbles and to remove it from the acoustic signal obtained from the suspension to yield the underlying information about the suspended solid phase.

1.2 Objective of Research:

The objective of this study is to investigate the potential applicability of the acoustic probe to characterize solid-liquid and solid-gas-liquid slurries. In order to achieve this objective it is necessary develop a forward theory to predict the acoustic response of a solid-liquid slurry, given an *a priori* knowledge of its microstructure, which can then be compared with experimental results. To be practical, the theory must include consideration of both dilute and concentrated slurries. Further, it is desired to develop an inverse theory to determine the solids concentration and volume fraction distribution in a solid-liquid slurry from its experimentally obtained acoustic response. Lastly, it is desired to extend the forward theory for solid-liquid systems to solid-gas-liquid slurries and compare theory predictions with experimental results for these systems.

1.3 Organization of Dissertation:

The work presented in this study consists of four main areas of investigation which are discussed separately in individual chapters. The experimental data in each area of study are acquired by slight variations of two main experimental techniques. Chapter 2 gives a literature survey of experimental techniques which are especially relevant to this study. Chapter 3 describes the experimental equipment, instrumentation, and procedures employed in this study. Chapter 4 presents theory and a comparison with experimental data of the attenuation of acoustic waves in dilute solid-liquid suspensions. Chapter 5 examines the inverse problem to determine the solids concentration and particle size distribution in solid-liquid slurries. In Chapter 6 a theory is presented for predicting the

attenuation of acoustic waves in concentrated slurries, and the predictions of the theory are compared with experiments. Chapter 7 gives the preliminary results of attenuation measurements in solid-gas-liquid slurries. Finally, conclusions and recommendations for future work are given in Chapter 8.

Chapter 2: Literature Survey

2.0 Introduction to Literature Review:

It is the goal of this chapter to present a literature review of experimental techniques which are relevant to the work performed in this investigation. Only literature pertaining to the experimental studies is presented here. The literature surveys related to the various theories are presented in the respective chapters in which they are relevant.

2.1 Ultrasonic Experimental Techniques:

2.1.1 Measurements Techniques in Solid-Liquid Systems:

Experimentation using ultrasound techniques has been going on for quite some time. Urick (1947 and 1948), for example, measured the velocity and attenuation of ultrasound in solid-liquid suspensions in two different experimental studies using a fairly simple ultrasound interferometer which consisted of a "bare" quartz (piezoelectric) crystal and relatively simple electronics operated in a pulse-echo mode. Since that time, many other investigators have made attenuation and/or phase speed measurements in solid-liquid suspensions using more sophisticated instrumentation as technology, especially in the field of electronics, has advanced.

Allegra and Hawley (1972) used a semiautomatic version of the conventional pulse technique employed by Kessler *et al.* (1970) to measure attenuation as a function of frequency in suspensions of polystyrene spheres in water as well as in emulsions of

toluene and hexane in water. They observed that the attenuation data obtained from the liquid-liquid emulsions by their technique yielded good agreement with predictions made by the theory of Epstein and Carhart (1953). They also extended the Epstein and Carhart theory to solid-liquid suspensions and observed good agreement between the theory predictions and experimental results.

Atkinson (1991) used a commercially available 1.0 MHz immersion transducer (Panametrics Model V302) as a transmitter and a custom made polyvinylidene fluoromer (PVDF) receiver to perform phase speed and attenuation measurements in packed beds and fluidized beds of 1.0 mm glass beads in water. Atkinson (1991) reported that the advantage of using the piezoelectric polymer, PVDF, as the acoustic receiver was that it could be custom made into virtually any size, and that PVDF hydrophones have fairly flat acoustic response in the range of DC (implying zero frequency) to several Megahertz.

Alba (1992) patented an at-line (next to the process line) device which measures concentration and size distribution of particles in suspensions. It employed piezoelectric transducers mounted in tubes in a vessel wall allowing for variable distance between transducers through a sliding contact. The input signal to the transmitter transducer was a continuous wave transmitted for a few milliseconds at a time. Attenuation measurements were then made at two or more separation distances. This device is reported to be applicable to solid-liquid slurries containing particles ranging in size from 0.01 to 1,000 μm at concentrations from 0.1 % to 70 % by volume. The particle size distribution is determined by fitting the resulting measured attenuation spectrum to one calculated from an *a priori* assumed distribution, such as log-normal or Gaussian. The main

disadvantages of this device are that it requires a knowledge of the materials which constitute the slurry and the assumption that the particle population can be described by a commonly known type of size distribution.

Greenwood *et al.*(1993) employed two piezoelectric transducers of 2.25 MHz centerline frequency separated by four inches in a tank to measure the attenuation as a function of frequency from 0.5 to 3.0 MHz in a kaolin/water slurry for solids volume fractions up to 0.24. The transmitter transducer was driven by signals from a toneburst swept frequency generator. Measurements were made by photographing the voltage versus frequency of the signal received which was displayed on an oscilloscope screen for each slurry concentration studied and comparing the voltage values at six individual frequencies for each concentration with the corresponding values in water. The attenuation was then calculated from ratios of the slurry voltages at each frequency to those in water at the same frequency. It was observed that the attenuation is proportional to the frequency and solids volume fraction within the investigated ranges of these parameters. These results further demonstrated that it is feasible to use attenuation measurements to determine the solids concentration in slurries.

2.1.2 Measurement Techniques in Liquid-Liquid Dispersion and Emulsions:

Much work has been done in the monitoring and characterization of liquid-liquid dispersions using an ultrasonic technique. Bonnet and Tavlarides (1987) developed an ultrasonic technique which used the time-averaged model of Kuster and Toksoz (1974) to

predict the dispersed phase volume fraction in liquid-liquid dispersions and suspensions based on the difference in travel time of the ultrasound in the pure materials and in the dispersion. This technique was later improved to account for effects of the dispersed phase (such as the sphericity and polydispersity of the drops) on the travel time by modifications to the time-averaged model (Yi and Tavlarides 1990; Tsouris and Tavlarides 1990; Tsouris and Tavlarides 1993). These modifications allowed the technique to be employed under conditions of large dispersed phase volume fraction and in situations where the velocity of sound was greater in the organic phase than in the aqueous phase. These improvements in the ultrasonic technique eventually led to the development of a miniaturized, in-situ pulse-echo ultrasonic probe to measure local dispersed phase volume fraction in liquid-liquid dispersions (Tsouris *et al.* 1995), which was also shown to have the capability to detect phase inversion in these dispersions.

McClements (1992) measured ultrasound velocity and attenuation coefficients in 10 wt % emulsions of *n*-hexadecane in water using a device called a Frequency Scanning Ultrasonic Pulse-Echo Reflectometer (FSUPER). This device measured the amplitude and phase differences, through Fourier analysis, between signals transmitted through a Perspex buffer rod in the sample cell and the buffer rod plus emulsion sample. McClements (1992) observed good agreement between the data obtained in that study and multiple scattering theory for dilute emulsions of dispersed phase volume fraction less than 0.13. However, there was some deviation from the multiple scattering theory for more concentrated emulsions, especially at low frequencies and small drop sizes. McClements (1992) suggested that this deviation between theory and experiment could

be due to interaction between the drops, which is not included in the multiple scattering theory. Another suggested source of discrepancy was interference with the measurement by the incoherent part of the scattered signal.

2.1.3 Measurement Techniques in Three-phase Systems:

Okamura *et al.* (1989) and Uchida *et al.* (1989), in two related works, used the degree of phase difference between acoustic signals obtained in liquid, solid-liquid, and three phase systems to empirically determine the concentration of solids in three phase reactors. The main premise of their work was that the presence of the gas phase did not affect the phase shift of the signal received which was induced due to the presence of the solid particles alone. Therefore, one could determine the solids concentration in a three phase slurry simply by measuring the phase lead in the signal received. This technique is successful because the transmitted signal never actually encounters any of the gas phase. When the transmitted signal does encounter gas bubbles, it is completely blocked. So the signals upon which the measurements are made are only signals acquired when no gas bubbles are encountered. Therefore, this technique is essentially measuring the solids hold up in a two phase system.

Soong *et al.* (1995) used a technique based on that of Okamura *et al.* (1989) to perform ultrasonic measurements of the solids concentration in a three phase slurry consisting of water, nitrogen bubbles, and glass beads. Particular attention was placed on the effects of the gas flow. The bubbles were estimated to be of the order of 3 to 5 mm in size. The authors concluded that the attenuation is slightly affected by the gas flow rate,

and the transit time of the ultrasonic signal is not affected by the gas flow rate. Both the amplitude ratio and the travel time were affected by the solids concentration.

Soong *et al.* (1996) performed similar measurements in three phase slurries of molten paraffin wax, nitrogen bubbles, and glass beads. In this study, the bubble size was also about 5 mm. This study concluded that both the amplitude and the transit time of an ultrasonic signal were influenced by the variation of solids concentration in paraffin wax. It was, again, found that the variation of nitrogen flow had very little effect on the observed transit times. The gas probably did not have a great effect on the measurements because of the bubble size. Bubbles in the size range of 3 to 5 mm have extremely low resonance frequencies (about 1 kHz). Therefore, the measurements were made at frequencies well beyond the bubble resonance frequency. Bubbles of this size would only affect the transmitted signal if they were present in a large enough concentration to completely block the signal. These techniques are successful because the experimental conditions are such that the gas phase is not really relevant to the measurements.

2.2 Bubble Generation Techniques in Acoustic Studies:

Carstensen and Foldy (1947) conducted measurements of the transmission, scattering and reflection of sound by screens of bubbles. The bubbles were generated by a novel device called a microdisperser. This apparatus consisted of two concentric glass tubes. The inner tube was of capillary dimension (0.01 cm i.d.), and it carried air at approximately 0.5 to 2.5 psi above the hydrostatic pressure at its terminus. The outer tube directed a flow of water over the inner capillary tube. The effect of the water flow

was to strip air bubbles away from the capillary tube end as soon as they formed. Coarse control of the bubble size was provided by varying the water flow rate, and bubbles were generated in the size range of approximately 100 to 400 μm.

Silberman (1957) measured the attenuation and phase speed of sound in bubbly liquids by establishing standing waves in steel pipes filled with a gas-water mixture. The attenuation was then determined from pressure measurements. The bubbles in this study were produced by pumping gas at extremely small flow rates through hypodermic needles and other small diameter tubing. This procedure consistently produced bubbles with diameters of 1 to 3 mm at approximately 1 % by volume. The Silberman (1957) study is considered significant because of its superior control of the bubble size and the accuracy of the data which generally agreed well with the theory, except in the immediate neighborhood of bubble resonance.

Kol'tsova *et al.* (1979) measured the excess attenuation in liquids containing between 0.025 % and 0.02 % (by volume) of small hydrogen bubbles. The bubbles were created by electrolysis. The cathode of the electrolyzer consisted of 0.02 mm diameter copper wire wound around rectangular Bakelite plates at a spacing of 1 to 3 mm. Several plates were stacked together with the wire turns interconnected on one side. The wire turns on the opposite side were polished such that the wires were severed to form stubs from which the bubbles emanated. The anode was a thin platinum wire stretched above the cathode. A 3 % NaCl solution was hydrolyzed to create bubbles with radii in the range of 7 to 45 μm. These bubble sizes are much smaller than those described in

previous investigations, and they are the approximate bubble sizes which are of interest in the present study.

2.3 Photomicrographic Imaging Techniques:

Photomicrographic techniques of various types have been employed rather widely in the past to measure particle, bubble, and drop sizes in a vast array of dispersed phase systems. For example, Kirou *et al.* (1988) employed a photomicrographic technique, which was a modification of that developed by Bapat (1982), to measure droplet size in an Oldshue-Rushton extraction column. This method consisted of a microscope tube interfaced with a 35 mm camera. The microscope objective viewed the droplets through a special window port in the wall of the extraction column which was designed to prevent droplets from passing between the objective lens and those droplets in the objective's focal plane. Backlighting was provided by a rigid fiber optic light conduit which also passed through the port and was bent to face the photographic window. The light conduit was coupled to a microflash unit which was synchronized to the camera shutter. Droplets were photographed as they passed between the fiber optic conduit and the window, and their sizes were measured using a semi-automatic technique.

Kol'tsova *et al.* (1979) employed a photographic technique to measure the size distributions of microbubbles in their study of the attenuation of ultrasound in bubbly liquids. Although not many details of the bubble size measurements are provided, it seems that the bubbles were either photographed or viewed visually through optical glass windows in the walls sample test cell with the aid of a long distance microscope.

Pacek *et al.* (1994) employed a video technique to study the dynamics of phase inversion in liquid-liquid dispersions. Their technique allowed for the collection of data on the transient mean drop size and the transient drop-size distribution during phase inversion. The system of Pacek *et al.* (1994) consisted of a stereo microscope with a very shallow depth of field attached to a high speed video camera. Sharp images of dispersed phase drops were captured by using a strobotach synchronized with the video camera at its framing rate. Pacek *et al.* (1994) were able to photograph dispersed phase droplets of sizes of 40 μm and larger for accurate measurements at dispersed phase concentrations of up to 70 % by volume. The photographs were analyzed semiautomatically via computer to yield cumulative and frequency drop size distributions to any mean size.

Tsouris *et al.* (1995) employed a high speed imaging system to visualize drops produced at the tip of the nozzle of an electrostatic spraying apparatus. This system consisted of a Kodak Ektapro Intensified Imager which had a maximum frame speed of 12,000 frames per second. The imager was connected to a video recorder, a monitor, and a printer. This system was employed to measure large drops (approximately 0.5 to 2.5 mm diameter) of TCE (trichloroethylene) electrostatically sprayed into water.

Burns *et al.* (1997) used a video based digital imaging system to measure sizes of bubbles generated by various techniques such as electrolysis (electroflotation), electrostatic spraying, and dispersed air flotation (DAF). An image analysis system was employed to measure the equivalent circular diameter of the bubbles produced. The hardware employed depended upon the size of the bubbles produced. For the techniques which produced relatively large bubbles (diameters larger than about 100 μm in diameter), the bubbles were

photographed by a high speed video camera fitted with a magnifying lens. Smaller bubbles (less than approximately 100 μm in diameter) were photographed with the video camera interfaced with a long distance microscope capable of magnification of up to 230 to 250 times. The camera in each set up was interfaced to a video recorder, a monitor, and a printer. A light source was set up behind the test cell, shining toward the camera so that the bubbles appeared as dark images on a light background. The image analysis system consisted of a control computer and software which measured the area of individual bubbles and converted it to an equivalent circular diameter. The calibration factor for the bubble size measurements was determined by videotaping and measuring a wire of known diameter. The identical imaging system was used by Shin *et al.* (1997) to measure sizes of bubbles produced in experiments involving the electrostatic spraying of air into water.

Chapter 3: Experimental Studies

3.1 Experimental Equipment:

It should be noted that a number of combinations of transducers, mixing vessels and test cells, and experimental techniques were employed to obtain the attenuation data presented in this study. Therefore, in the caption of each figure which presents attenuation data obtained in this study, there is an "experimental parameter number". This number begins with a capital letter "E" (indicating experimental parameter series) and is followed by four numbers. Each of the four numbers refers to a particular set of parameters used in the experiments to yield that data set. The key to extracting the specific experimental parameters from the experimental series number is given in Appendix D.

3.1.1 Mixing Vessels and Test Cells:

Initial Experiments in solid-liquid systems in this study have been conducted in a cylindrical polyvinyl chloride (PVC) vessel of approximately 3.9 L in volume with 15.5 cm I.D. and 20.5 cm height. Four transducer ports spaced at 90^{0} allow for the employment of two transducer pairs in each experimental "run". A "false bottom" can be inserted into the vessel to allow for a smaller sample volume of 1.6 L.

Also, various other vessels are employed depending upon the nature of the system to be interrogated. In instances where the materials under consideration are quite

expensive (such as polystyrene spheres) allowing only small slurry volumes, or the volume fraction of solids is high making suspension difficult, Plexiglas test cells of rectangular "box" geometry and various nominal transducer separation distances are employed. There are four different test cells with nominal transducer separation distances of 1.27 cm, 2.54 cm, 5.08 cm, and 10.2 cm. A schematic diagram of a Plexiglas test cell is shown in Figure 3.1. These cells are designed to accommodate only a small sample volume while still being large enough to avoid the effects of signal reflection off the cell walls due to spreading of the transmitted ultrasound beam as described in Kinsler *et al.* (1982). When these test cells are used, the suspension of the slurry is provided through manual agitation with a glass stirring rod.

3.1.2 Ultrasonic and Accompanying Electronic Equipment:

In regard to electronic equipment, there are two distinct experimental set-ups which are employed. The first setup is shown in Figure 3.2, and it is based on an experimental system employed by the Non-Destructive Evaluation Section of the Energy Division at the Battelle Pacific Northwest National Laboratory. This system consists of a desktop computer with a Matec TB-1000 digital synthesizer card capable of generating monochromatic tonebursts from 0.05 to 20 MHz in frequency. An example of a 1 MHz toneburst in both water and a 5% soda lime glass slurry is shown in Figure 3.3. A toneburst of a given frequency is sent to the transmitter piezoelectric transducer (Panametrics Videoscan Immersion Transducers Models V391, V302, V304, V308, V320, and V311), through the medium (either water or slurry), to the receiver transducer.

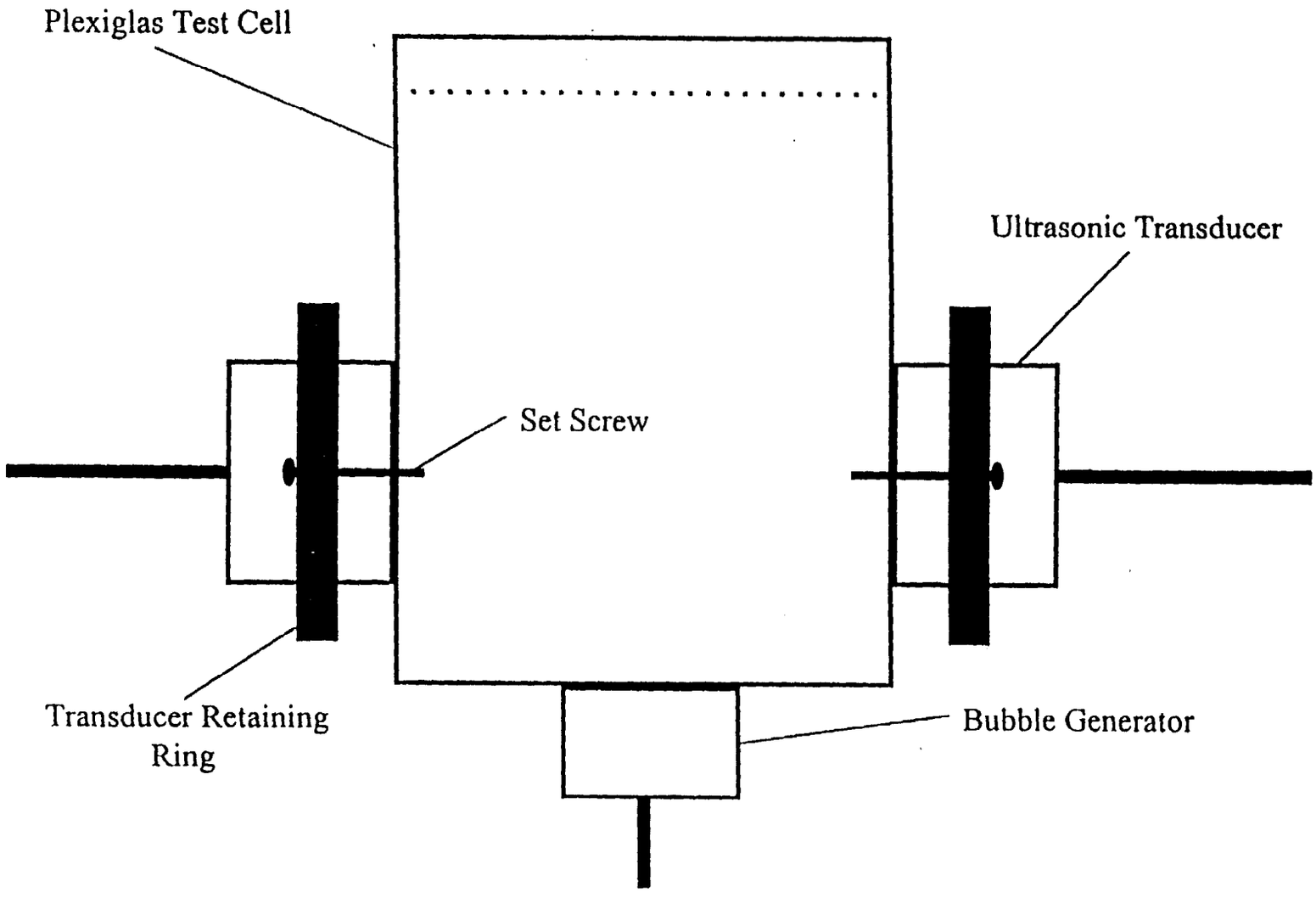

Figure 3.1: Schematic diagram representing five different Plexiglas test cells employed in the solid-liquid and solid-gas-liquid experimentation.

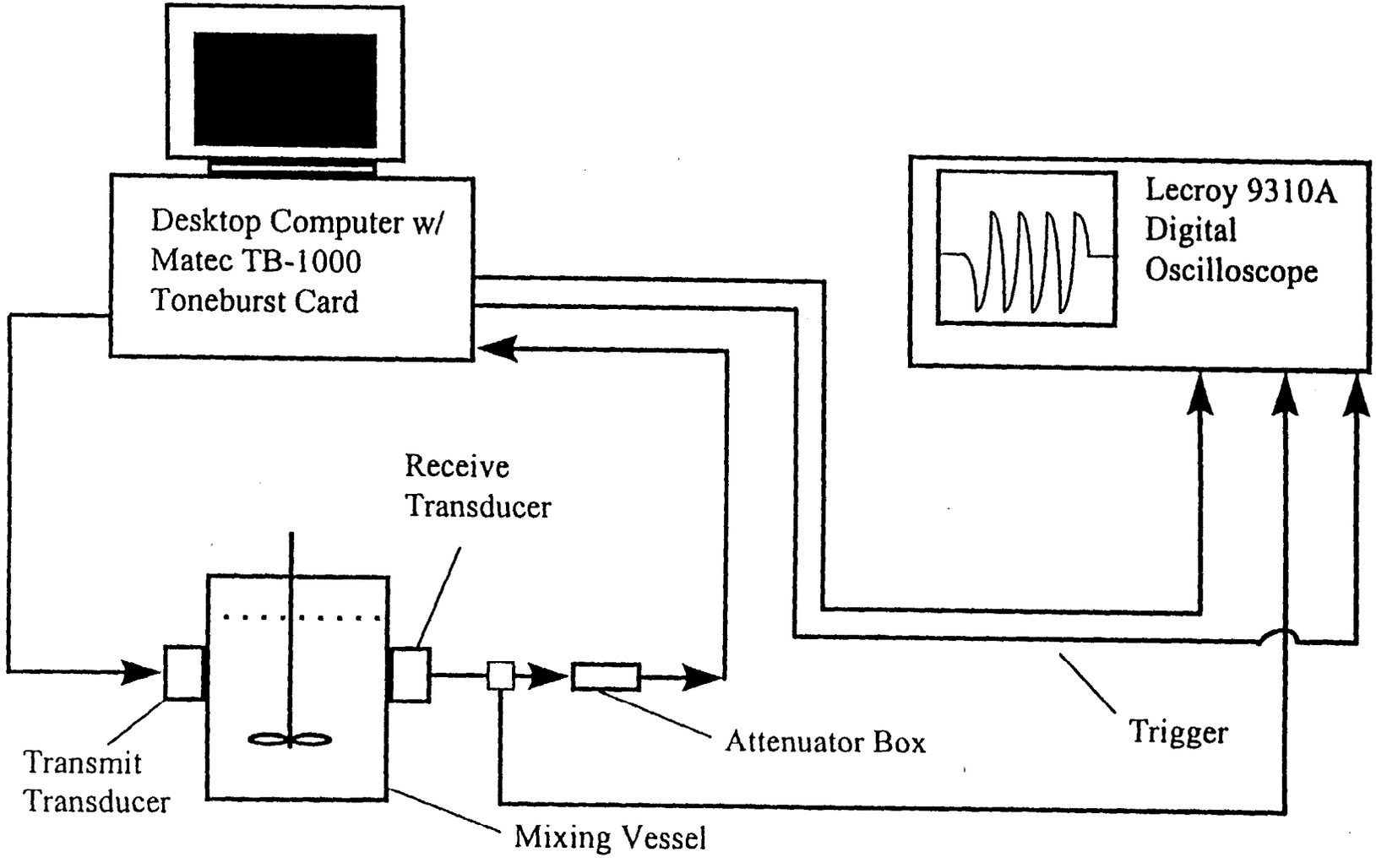

Figure 3.2: Schematic diagram of the experimental set-up used in the Toneburst Technique.

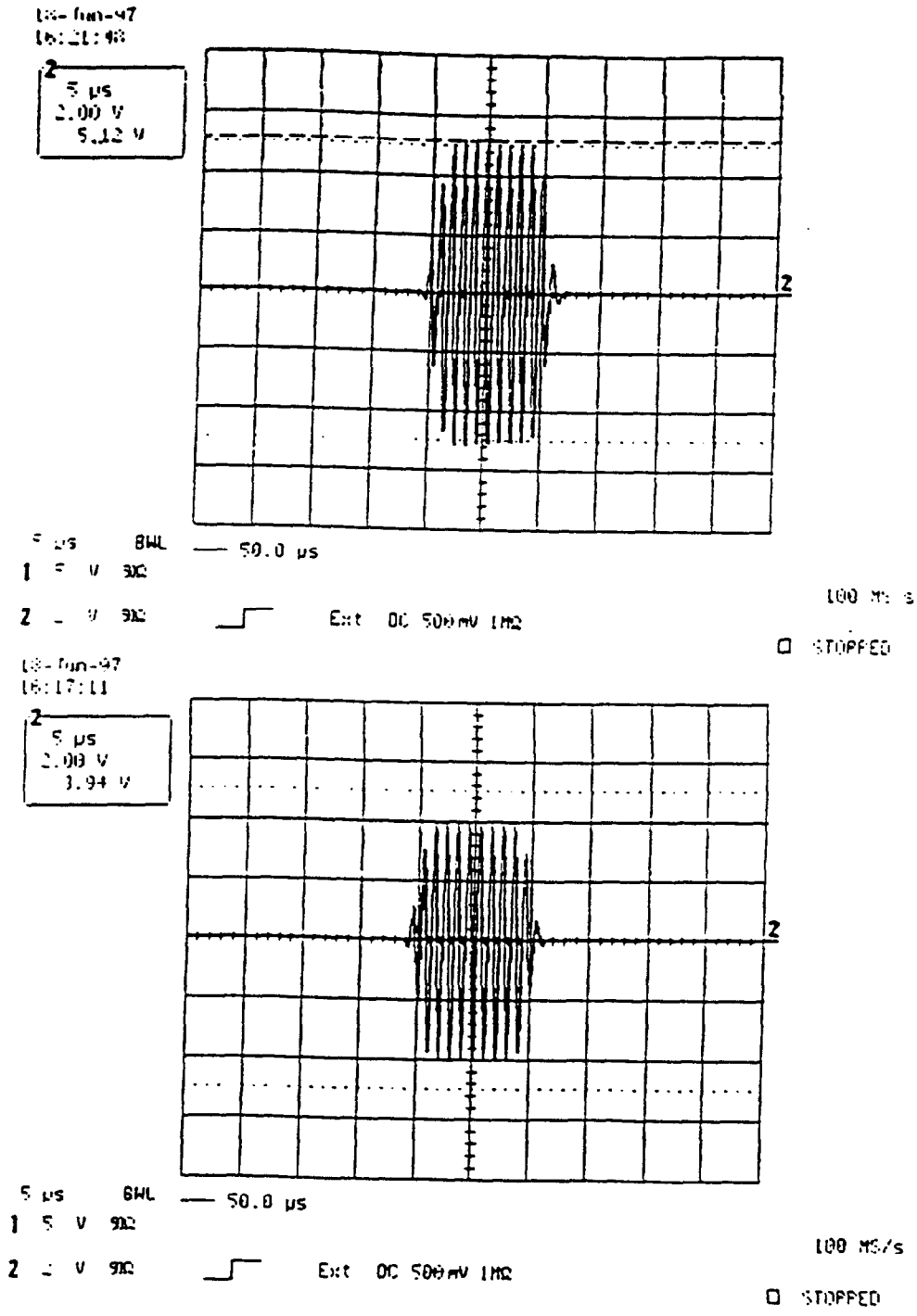

Figure 3.3: Oscilloscope traces for a 1.0 MHz toneburst transmitted through distilled water and through a 5 % by volume soda-lime glass slurry.

The technical specifications associated with each transducer used in this study, including transducer bandwidth, are given in Table 3.1. A discussion of the determination of transducer bandwidth is given in Appendix E. The received signal can be either sent through the built in amplifier (capable of amplification from 0 to 70 dB) on the toneburst card (via a Pasternak Enterprises No. PE7008-1 50 Ohm attenuator box, if necessary) to a LeCroy Model 9310A digital oscilloscope, or directly to the oscilloscope where the amplitude of the received toneburst is measured. The amplitude data are then entered into computer data files which are then loaded into a MATLAB™ code which, after correcting for attenuator and amplifier settings, calculates the attenuation, α (in Np/cm), according to the formula:

$$\alpha = -\frac{1}{d}\log\left(\frac{V_{\text{mix}}}{V_{\text{H}_2\text{O}}}\right), \qquad (3.1)$$

where d is the distance (in cm) between the transducers, and V_{mix} and V_{H2O} are the voltage amplitudes of the signals received in the mixture and pure water, respectively. It should be noted that the term "log" in equation (3.1) refers to the natural logarithm. Various MATLAB™ codes written to manipulate the experimental data are shown in Appendix C.

The second experimental setup is similar to the first, but in this case the Matec TB-1000 card and computer are replaced by a Panametrics Model 5052 PR Pulser/Receiver (cf. Figure 3.4). The pulser/receiver generates a negative spike pulse signal (instead of a toneburst) of 270 Volts which is sent to the transmitter transducer, propagates through the medium under investigation, and is received by the receiver transducer. The signal received then goes through the receiver which has an amplifier

Model #	Serial #	Element Diameter (cm)	Center Frequency (MHz)	Bandwidth (- 6 dB) (%)	Operating Range (MHz)
V391	226750	2.86	0.457	68.85	0.3 to 0.7
V391	228834	2.86	0.475	69.47	0.3 to 0.7
V302	211353	2.54	0.935	65.24	0.6 to 1.4
V302	211354	2.54	0.950	65.26	0.6 to 1.4
V304	217679	2.54	2.11	63.51	1.4 to 3.0
V304	217680	2.54	2.08	63.46	1.4 to 3.0
V308	219586	1.90	5.03	56.72	3.0 to 7.0
V308	219594	1.90	4.88	56.41	3.0 to 7.0
V320	222752	1.27	7.95	64.15	5.0 to 11.0
V320	222753	1.27	8.05	55.90	5.0 to 11.0
V311	221617	1.27	9.90	64.65	6.0 to 12.0
V311	221619	1.27	10.1	56.72	6.0 to 12.0

Table 3.1: Specifications for the Panametrics, Inc. (Waltham, MA) Videoscan immersion transducers employed in this study.